Structural Basis for the Synthesis of Indirubins as Potent and Selective Inhibitors of Glycogen Synthase Kinase-3 and Cyclin-Dependent Kinases

Panagiotis Polychronopoulos,[†] Prokopios Magiatis,[†] Alexios-Leandros Skaltsounis,*[,†] Vassilios Myrianthopoulos,[†] Emmanuel Mikros,[†] Aldo Tarricone,[‡] Andrea Musacchio,[‡] S. Mark Roe,[§] Laurence Pearl,[§] Maryse Leost,[||] Paul Greengard,[⊥] and Laurent Meijer*[,||,⊥]

Laboratory of Pharmacognosy and Laboratory of Pharmaceutical Chemistry, Department of Pharmacy, University of Athens, Panepistimiopolis Zografou, GR-15771 Athens, Greece, Structural Biology Unit, Department of Experimental Oncology, European Institute of Oncology, Via Ripamonti 435, 20141 Milano, Italy, 3, Centre for Structural Biology, Institute of Cancer Research, Chester Beatty Laboratories, 237 Fulham Road, London SW3 6JB, U.K., C.N.R.S., Cell Cycle Group, Station Biologique, B.P. 74, 29682 ROSCOFF Cedex, Bretagne, France, and Laboratory of Molecular & Cellular Neuroscience, The Rockefeller University, 1230 York Avenue, New York, New York 10021

Received September 1, 2003

Pharmacological inhibitors of glycogen synthase kinase-3 (GSK-3) and cyclin-dependent kinases have a promising potential for applications against several neurodegenerative diseases such as Alzheimer's disease. Indirubins, a family of bis-indoles isolated from various natural sources, are potent inhibitors of several kinases, including GSK-3. Using the cocrystal structures of various indirubins with GSK-3β, CDK2 and CDK5/p25, we have modeled the binding of indirubins within the ATP-binding pocket of these kinases. This modeling approach provided some insight into the molecular basis of indirubins' action and selectivity and allowed us to forecast some improvements of this family of bis-indoles as kinase inhibitors. Predicted molecules, including 6-substituted and 5,6-disubstituted indirubins, were synthesized and evaluated as CDK and GSK-3 inhibitors. Control, kinase-inactive indirubins were obtained by introduction of a methyl substitution on N1.

Introduction

About 30% of human proteins contain covalently bound phosphate. Protein phosphorylation is considered to be one of the main posttranslational mechanisms used by cells to finely tune their metabolic and regulatory pathways. Protein kinases catalyze the phosphorylation of serine, threonine, and tyrosine residues of proteins, using ATP or GTP as the phosphate donor, while protein phosphatases are responsible for dephosphorylation, the opposite reaction. In view of the importance of phosphorylation in essentially all cellular and physiological events, it is not surprising that abnormal phosphorylation turns out to be a cause or consequence of numerous human diseases such as cancers, diabetes, and Alzheimer's disease (AD) (review in refs 1, 2). This is the reason screening for potent and selective inhibitors of protein kinases and phosphatases has intensified over the past few years (reviewed in ref 2−5). Presently three kinase inhibitors have been approved for clinical use, and more than 23 are undergoing clinical trials.[2]

Among the 518 human kinases,[6] two classes have been particularly explored, namely the cyclin-dependent kinases (CDKs) and glycogen synthase kinase-3 (GSK-3). Some CDKs (such as CDK1, 2, 4, 6) control progression through the cell division cycle and apoptosis and appear to be deregulated in many human cancers (review in ref 7−9). Other CDKs (CDK5, CDK11) are involved in various functions in the nervous system. CDK5 is abnormally regulated in AD and other neurodegenerative disorders (reviewed in ref 10−12). GSK-3 is involved in programmed cell death, in tumorigenesis, in diabetes, [13] and in AD (reviewed in ref 14−16). Interestingly, CDK5 and GSK-3 are two main kinases involved in the abnormal hyperphosphorylation of the microtubule-binding protein tau, one of the diagnostic features of AD. Recently, it was demonstrated that transgenic mice coexpressing both mutant human (P301L) tau and p25, the CDK5 activator, show an accumulation of aggregated, hyperphosphorylated tau, associated with GSK-3, and increased neurofibrillary tangles.[17] Recent studies also established that GSK-3 is involved in the production of amyloid-β peptides,[16,18] another event thought to be directly involved in AD's development. These observations constitute strong encouragement for the search for GSK-3/CDK5 inhibitors as potential pharmacological agents to treat AD.

Over the past decades a fair number of potent and selective pharmacological inhibitors of CDKs (reviewed in 19−22) and GSK-3 (reviewed in refs 23−24) have been identified and characterized. Interestingly, many inhibitors (but not all) are in fact dual inhibitors of CDKs and GSK-3, acting through competition with ATP binding.[25] Among these inhibitors are indirubins,[25,26] a family of bis-indoles extracted from various natural sources such as indigo-producing plants (reviewed in ref 27), several species of Gastropod mollusks (reviewed in ref 28), urine in healthy and diseased patients (ref 29 and references therein), and various wild-type or re-

* Corresponding authors: A. L. Skaltsounis (tel: +3210 7274598, fax: +3210 7274594, e-mail: skaltsounis@pharm.uoa.gr) or L. Meijer (e-mail: meijer@sb-roscoff.fr).
[†] University of Athens.
[‡] European Institute of Oncology.
[§] Chester Beatty Laboratories.
[||] C.N.R.S.
[⊥] The Rockefeller University.

10.1021/jm031016d CCC: $27.50
Published on Web 01/08/2004

combinant bacteria (reviewed in refs 30, 31). Indirubins are recognized as the main active ingredient of a traditional Chinese medicinal recipe, Danggui Longhui Wan, used to treat chronic myelocytic leukemia (reviewed in refs 32, 33). Indirubins have clear antiproliferative effects. [34,35] These effects may be accounted for by inhibition of CDKs and GSK-3, but also by interaction with the aryl hydrocarbon receptor (AhR) [29] (Knockaert et al., submitted). Also known as the "dioxin receptor", this orphan receptor plays a poorly defined role in cell cycle control (reviewed in ref 36). Its deregulation leads to the appearance of stomach tumors.[37] AhR agonists have been reported to block cell proliferation, and some are being considered for antitumor treatment.[38−40]

The pharmacological potential of indirubins prompted us to investigate other natural sources for novel indirubin analogues. In this context we focused our efforts on "Tyrian purple" or "Royal Blue", a vivid purplish red dye extracted since antiquity from Gastropods of the *Muricidae* and *Thaididae* families and constituted of a mixture of various brominated indigos and indirubins. The identification of 6-bromoindirubins as potent, selective inhibitors of GSK-3 (Meijer et al., submitted) led us to investigate this subclass of indirubins. Aided by the cocrystal structures of various indirubins with CDK2,[26] CDK2/cyclin A,[41] CDK5/p25, and GSK-3β (Meijer et al., submitted), we analyzed and modeled the binding of indirubins within the ATP-binding pocket of these kinases. This modeling approach allowed us to understand the molecular basis for selectivity and to predict improvements of the indirubin family as kinase inhibitors. Predicted molecules were synthesized and evaluated as CDK and GSK-3 inhibitors.

Results

Indirubins have been cocrystallized successfully with CDK2,[26] CDK2/cyclin A,[41] and recently with CDK5/p25 and GSK-3β (Meijer et al., submitted) and the *Plasmodium falciparum* kinase *Pf*PK5 (Holton et al., submitted). In all cases indirubins are inserted in the ATP-binding pocket located between the small and large lobes of the kinases (Figure 1a−d). Comparison of the different structures shows that indirubins adopt a very similar orientation in this enclosed environment. We have taken advantage of the availability of these cocrystal structures and of substantial kinase inhibition data for a large set of indirubin analogues to initiate a quantitative SAR study and to predict further improvements in the potency and selectivity of indirubins as kinase inhibitors.

Chemistry

Synthesis of Indirubin Derivatives. The high selectivity for GSK-3 of 6-bromoindirubin and 6-bromoindirubin-3′-oxime (Meijer et al., submitted) prompted us to investigate more extensively the role of the substituent at position 6. In addition, the high inhibitory activity against various CDKs of the previously described indirubin derivatives [25] substituted at position 5 led our interest to a series of bisubstituted indirubins, namely on positions 5 and 6, thereby possibly combining selectivity and high activity. These latter compounds were predicted prior to synthesis according to the model described in the molecular modeling section.

The synthesis of 6-monosubstituted or 5,6-bisubstituted indirubins was mainly based on the dimerization reaction of an appropriately substituted isatin derivative with 3-acetoxyindole, as depicted in Scheme 1, except in the case of 6-vinylindirubin which was prepared directly from 6-bromoindirubin employing the Stille reaction. The desired isatins were synthesized through a two-step procedure,[42] using the corresponding commercial mono- or bisubstituted anilines **1a**−**f** as starting material. In the first step, the appropriate aniline derivatives were reacted with chloral hydrate and hydroxylamine hydrochloride to give the corresponding isonitrosoacetanilides **2a**−**f**. In the second step, the intermediate isonitrosoacetanilides were heated in concentrated sulfuric acid to give a mixture of **3a**−**f** and **4a**−**f**. The separation of that mixture was based on the fractional decantation of the corresponding isatin sodium salts with acetic acid or hydrochloric acid.

6-Bromo-5-nitroisatin (**3g**) was not synthesized from the corresponding aniline, which was not commercially available, but by selective nitration of the easily obtained 6-bromoisatin (**3a)** with $NaNO_3$ in H_2SO_4.[43] 6-Bromo-*N*-methylisatin (**11a**) and *N*-methylisatin (**11b**) were prepared from **3a** or isatin by treatment with dimethyl sulfate and Na_2CO_3 (Scheme 2).

The substituted isatins **3a**−**g**, isatin (**3h**), 6-bromo-*N*-methylisatin (**11a**), and *N*-methylisatin (**11b**) were reacted with 3-acetoxyindole (**10b**) in alkaline medium to give, generally in good yields the corresponding bisindoles **5a**−**h, 12c,** and **12d** selectively in a *Z* form**.**[42] This reaction was generally problematic in the case of the 4-substituted isatins **4a**−**f** due to stereochemical hindering and the distortion caused by the substituent in position 4. A poor yield (5%) could only be achieved in the case of **4d** where the substituent was a chlorine atom. Complete failure of the reaction was observed in the case of more bulky substituents such as bromine or iodine.

A similar dimerization reaction was employed for the synthesis of 6′-bromoindirubin (**12a**) and 6,6′-dibromoindirubin (**12b**) which were prepared from isatin (**3h**) or 6-bromoisatin (**3a**) and 6-bromoacetoxyindole (**10a**), respectively, as depicted in Scheme 2. 6-Bromoacetoxyindole (**10a**) was prepared from 6-bromoisatin in five steps as previously described.[42]

As already mentioned, 6-vinylindirubin (**5i)** was prepared in very good yield employing the Stille reaction. 6-Bromoindirubin (**5a**) was used as starting material, tributylvinylstannate as the vinyl group donor and tetrakis(triphenylphosphine)palladium as catalyst.

The oximes**7a**−**i** and **13a**−**d** were prepared selectively in a (2′*Z*,3′*E*) form following a typical procedure from the appropriate indirubin derivatives **5a**−**i** and **12a**−**d** with hydroxylamine hydrochloride in pyridine under reflux. A similar typical procedure was followed for the preparation of the methoximes **9a** and **9b** from **5a** and **5h** using methoxylamine hydrochloride. The acetoximes **8a**−**i** and **14** were prepared from the oximes **7a**−**i** and **13c** with acetic anhydride in pyridine. The temperature of the reaction was carefully kept at 0 °C to avoid bisacetylation.

Biological Tests

Indirubin analogues were tested against three protein kinases, CDK1/cyclin B, CDK5/p25, and GSK-3α/β. All

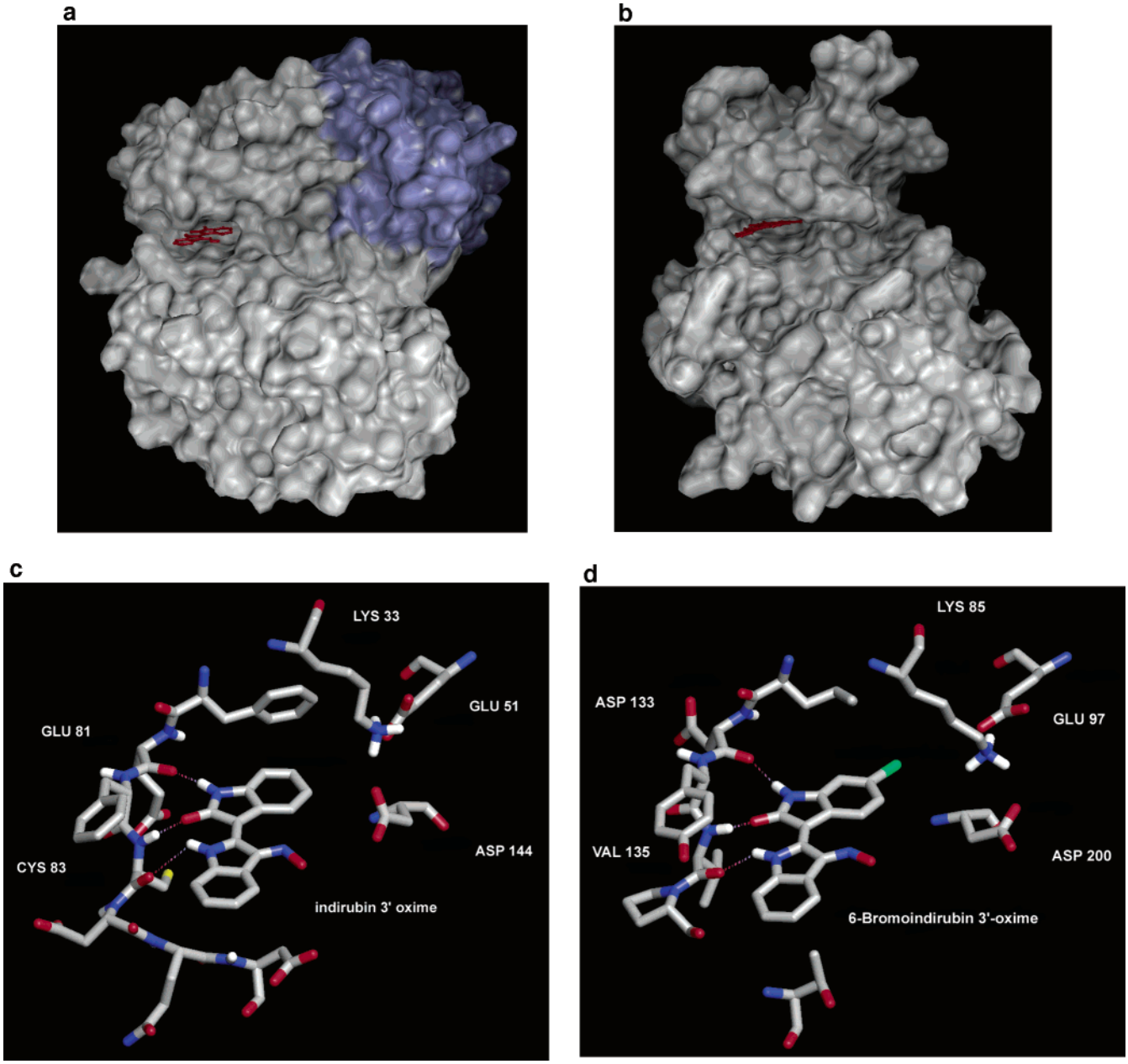

Figure 1. Crystal structure of indirubin-3′-oxime in complex with CDK5/p25 (a, c) and of 6-bromoindirubin-3′-oxime with GSK-3β (b, d). Inhibitors bind in the ATP-binding pocket of the catalytic site, mainly through hydrophobic interaction and three hydrogen bonds with Cys 83 and Glu 81 (CDK5) or Val 135 and Asp 133 (GSK-3 β). Indirubins are shown as ball-and-stick models. The figures were created with the molecular viewer of AutoDockTools and Macromodel. For details on CDK5/p25 crystal structure see ref 51.

assays were run in the presence of 15 μM ATP and appropriate protein substrates (histone H1 for CDKs, GS-1 peptide for GSK-3). IC_{50} values were determined from dose−response curves and are provided in Table 1.

Although the cocrystallization studies have been performed with CDK2, we have used CDK1/cyclin B rather than CDK2 for the screening because of a practical reason: CDK1/cyclin B is available as the native enzyme and is extracted and purified from starfish oocytes. It is extremely active and not contaminated by inactive complex nor by inactive monomers. In contrast CDK2/cyclin-E is only available as a recombinant enzyme, thus partially contaminated with inactive enzyme (poorly folded, monomers, partially phosphorylated, etc.). We have thus chosen to use the native rather than the recombinant enzyme. In any case CDK1 and CDK2 only differ by two amino acids in the ATP-binding pocket. Furthermore, all CDK1 inhibitors we have uncovered are equally active on CDK2.

Molecular Modeling

To gain better insight into the interactions between the various synthesized compounds and GSK-3β, we performed molecular mechanics docking−scoring calculations. The relative biological activity was correlated with the calculated interaction energy, and a model was constructed allowing the prediction of the affinity of indirubin analogues prior to synthesis. Binding affinities were estimated using PrGen v.2.1 software,[44] evaluating ligand−receptor interaction energies, ligand desolvation energies, and changes in both ligand internal energy

Scheme 1[a]

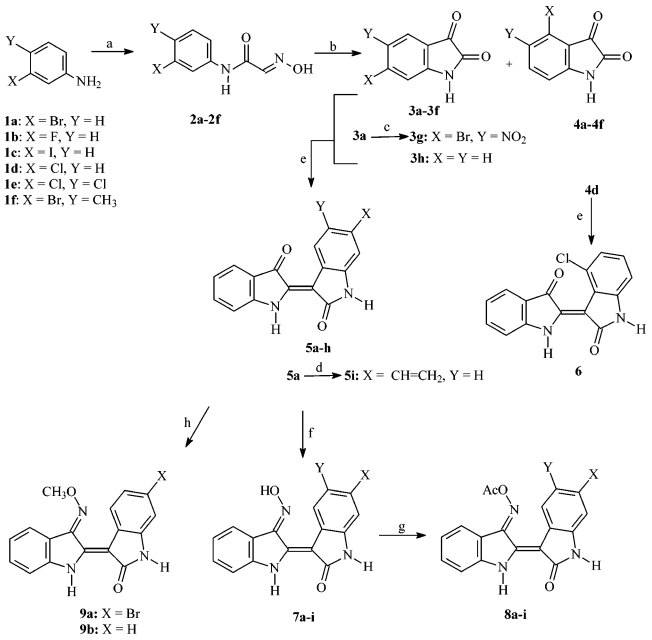

[a] Reagents: (a) chloral hydrate, Na_2SO_4, $H_2NOH{\cdot}HCl$, H_2O, H^+; (b) H_2SO_4; (c) $NaNO_3$, H_2SO_4, 0 °C; (d) $[CH_3(CH_2)_3]_3SnCH{=}CH_2$/$[(C_6H_5)P]_4Pd$, dioxane, 100 °C; (e) 3-acetoxyindole, Na_2CO_3MeOH, 25 °C; (f) $H_2NOH{\cdot}HCl$, Py, 120 °C; (g) Ac_2O, Py, 0 °C; (h) $H_2NOCH_3{\cdot}HCl$, Py, 120 °C.

Scheme 2[a]

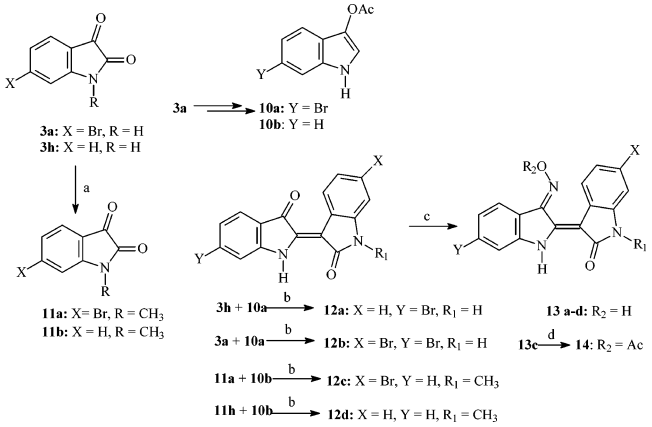

[a] Reagents: (a) $(CH_3)_2SO_4$, Na_2CO_3, DMF; (b) Na_2CO_3/MeOH, 25 °C; (c) $H_2NOH{\cdot}HCl$, Py, 120 °C; (d) Ac_2O, Py, 0°.

and ligand internal entropy upon receptor binding according to the formula:

$$E_{\text{binding}} \approx E_{\text{ligand-receptor}} - T\Delta S_{\text{binding}} - \Delta G_{\text{solvation,ligand}} + \Delta E_{\text{internal,ligand}}$$

Binding energies were coupled with experimental values in order to get a scoring function with high correlation. This was done through an iterative procedure implemented in PrGen referred to as the ligand equilibration protocol. It involved two steps: (a) correlation coupled receptor minimization and (b) unconstrained ligand relaxation/Monte Carlo search.

A training set of 23 molecules was subjected to ligand equilibration combined with Monte Carlo search. A total correlation coefficient of 0.902 and an RMS of 0.93 were achieved. The training set consisted of 11 previously described[25] molecules and 12 molecules described herein. The model was used to predict the activity of a test set of 15 molecules that were introduced within the equilibrated receptor cavity and subjected to Monte Carlo minimization. The resulting correlation between experimental and predicted binding affinities for both training and test sets is presented in Figure 2 while their ΔG and IC_{50} values are provided in Table 2. An excellent agreement between calculated and experimental values was observed with an RMS of 1.74. The largest deviation was obtained for 6-bromo-5-nitroindirubin, which was predicted to be 73 times more potent, while the other 14 ligands of the test set agreed within a factor of 8 or better.

The affinity of indirubins for GSK3 depends mainly on the hydrophobic van der Waals energy term which accounts for 66% to 92% of the sum of the three energy terms (VdW, electrostatics, H-bonding) as calculated by PrGen. The significance of VdW contributions on binding is also depicted in Figure 3a representing each energy term versus the total energy as varied throughout the different ligands. The total interaction energy values vary from −29 to −40 kcal/mol and the same is true for the VdW term (−25 to −39 kcal/mol) which appears to influence primarily the total energy. The contributions of the electrostatic (variation from −2 to −10 kcal/mol) and the H-bond term (variation from −0.3 to −6.7 kcal/mol) are of less importance and almost substituent independent. These latter two interactions, however, seem to be in most cases responsible for the improved affinity of the oxime-substituted indirubins when compared to their nonoxime analogues. The contribution of the electrostatic and HB term as expressed with the ratio (elect.+HB)/E_{total} was compared between 11 oximes and the corresponding nonoxime analogues (Figure 3b). In all cases except 6-F the ratio was greater in oxime analogues. No significant difference was observed concerning the contribution of VdW term (data not shown), suggesting that the =N−OH group stabilizing effect is of electrostatic character.

Discussion

Recent crystallographic data of CDK2,[26,41] CDK5 and GSK-3β (Meijer et al., submitted) in complex with various indirubins has provided valuable information on the active site differences along with specific interactions between those kinases and indirubin analogues. Substitution at position 6 turned out to be crucial for the selectivity while substitution at 3′ was found to be important for the binding affinity.

More specifically, in CDK5 and CDK2, the limits of the inner part of the binding cavity are defined by the side chain of Phe80 (Figure 1c) while in GSK-3 the corresponding residue is Leu132 (Figure 1d). The difference between the isobutyl side chain of Leu132 and the phenyl ring of Phe80 results in an increase of the pocket width in GSK-3 compared to that of CDK's (Figure 6) and can obviously explain the selectivity of 6-bromoindirubin toward GSK-3 compared to CDKs.

An important group of polar residues is located on the same side of the binding cavity: $Lys33^{CDK5}$/$Lys85^{GSK-3}$, $Asp144^{CDK5}$/$Asp200^{GSK-3}$, and $Glu51^{CDK5}$/$Glu97^{GSK-3}$, interacting with each other, together with substituents at C5 of indirubin. It has been proposed that these residues play an important role in the ligand−ATP

Table 1. Effects of Indirubins on Various Kinases[a]

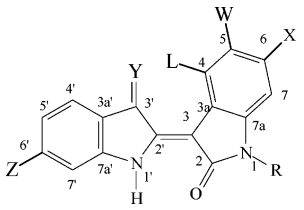

no.	compounds	X	Y	Z	W	L	R	CDK1/cyclin B	CDK5/p25	GSK-3α/β
5h	indirubin	H	O	H	H	H	H	10.000	10.000	1.000
7h	indirubin-3′-oxime	H	NOH	H	H	H	H	0.180	0.100	0.022
8h	indirubin-3′-acetoxime	H	NOAc	H	H	H	H	1.200	0.700	0.200
9b	indirubin-3′-methoxime	H	$NOCH_3$	H	H	H	H	1.000	0.400	0.150
12b	6,6′-dibromoindirubin	Br	O	Br	H	H	H	>100	>100	4.500
13b	6,6′-dibromoindirubin-3′-oxime	Br	NOH	Br	H	H	H	17.000	1.300	0.120
12a	6′-bromoindirubin	H	O	Br	H	H	H	>100	>100	22.00
13a	6′-bromoindirubin-3′-oxime	H	NOH	Br	H	H	H	3.000	1.200	0.340
5a	6-bromoindirubin	Br	O	H	H	H	H	>100	53.000	0.045
7a	6-bromoindirubin-3′-oxime	Br	NOH	H	H	H	H	0.320	0.083	0.005
8a	6-bromoindirubin-3′-acetoxime	Br	NOAc	H	H	H	H	63.000	2.400	0.010
9a	6-bromoindirubin-3′-methoxime	Br	$NOCH_3$	H	H	H	H	3.700	2.200	0.030
12c	6-bromo-*N*-methylindirubin	Br	O	H	H	H	CH_3	>100	>100	>100
13c	6-bromo-*N*-methyl-indirubin-3′-oxime,	Br	NOH	H	H	H	CH_3	92.000	>100	>100
5d	6-chloroindirubin	Cl	O	H	H	H	H	>100	>100	0.140
7d	6-chloroindirubin-3′-oxime	Cl	NOH	H	H	H	H	0.650	0.100	0.020
8d	6-chloroindirubin-3′-acetoxime	Cl	NOAc	H	H	H	H	30.000	0.200	0.017
5c	6-iodoindirubin	I	O	H	H	H	H	1.600	5.300	0.055
7c	6-iodoindirubin-3′-oxime	I	NOH	H	H	H	H	1.300	0.300	0.010
8c	6-iodoindirubin-3′-acetoxime	I	NOAc	H	H	H	H	2.200	1.300	0.013
5i	6-vinylindirubin	$CH{=}CH_2$	O	H	H	H	H	4.200	2.400	0.240
7i	6-vinylindirubin-3′-oxime	$CH{=}CH_2$	NOH	H	H	H	H	1.200	0.420	0.060
8i	6-vinylindirubin-3′-acetoxime	$CH{=}CH_2$	NOAc	H	H	H	H	1.600	0.400	0.065
5b	6-fluoroindirubin	F	O	H	H	H	H	1.500	1.000	0.650
7b	6-fluorooindirubin-3′-oxime	F	NOH	H	H	H	H	0.320	0.150	0.130
8b	6-fluoroindirubin-3′-acetoxime	F	NOAc	H	H	H	H	0.600	0.300	0.090
12d	*N*-methylindirubin	H	O	H	H	H	CH_3	>100	>100	>100
13d	*N*-methylindirubin-3′-oxime	H	NOH	H	H	H	CH_3	73.000	>100	>100
5f	6-bromo-5-methylindirubin	Br	O	H	CH_3	H	H	30.000	60.000	0.025
7f	6-bromo-5-methylindirubin-3′-oxime	Br	NOH	H	CH_3	H	H	0.300	0.130	0.006
8f	6-Bromo-5-methylindirubin-3′-acetoxime	Br	NOAc	H	CH_3	H	H	31.000	30.000	0.007
5e	6,5-dichloroindirubin	Cl	O	H	Cl	H	H	45.000	60.000	0.030
7e	6,5-dichloroindirubin-3′-oxime	Cl	NOH	H	Cl	H	H	0.140	0.060	0.004
8e	6,5-dichloroindirubin-3′-acetoxime	Cl	NOAc	H	Cl	H	H	30.000	0.100	0.004
5 g	6-Bromo-5-nitroindirubin	Br	O	H	NO_2	H	H	>100	>100	0.100
7 g	6-Bromo-5-nitroindirubin-3′-oxime	Br	NOH	H	NO_2	H	H	12.000	0.150	0.007
8 g	6-Bromo-5-nitroindirubin-3′-acetoxime	Br	NOH	H	NO_2	H	H	11.000	31.000	0.006
6	4-chloroindirubin	H	O	H	H	Cl	H	10.000	10.000	>100

[a] A series of indirubin analogues were tested at various concentrations in three kinase assays, as described in the Experimental Section. IC_{50} values (μM) were calculated from the dose−response curves.

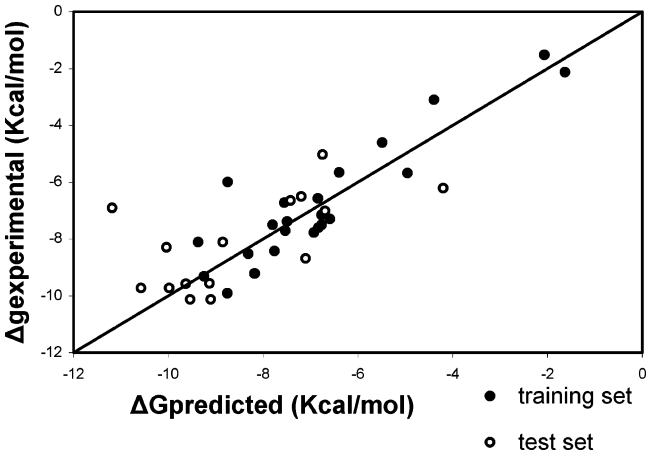

Figure 2. Correlation between experimental and predicted GSK-3β ΔG values of the indirubins. ○, training set; ●, test set.

recognition and affinity as Asp interacts with the phosphate hydroxyl group of ATP.[45] Moreover the interaction of these three residues could influence the position and flexibility of the Gly loop (residues 12−20) which closes over the end of the binding cleft.[41,46]

Additionally, the C3′ substituent seems to be important in the affinity as it has been noticed that the conversion of the C3′ carbonyl to an oxime improves inhibitory potency. The crystallographic structure cannot explain this enhancement by any obvious direct interactions of the oxygen or the hydrogen of the oxime with the receptor. A possible explanation could be an indirect interaction of this group with polar residue side chains through water molecules. More specifically it seems that a water molecule is conserved in approximately the same position in both crystal structures of both CDK5 (water 79) and CDK2 (water 49) interacting with the oxime group and the C3′ carbonyl oxygen respectively on one side and Asp86 on the other. Moreover this water molecule is located in the same position as the 4′-hydroxyl of ribose in the CDK2-ATP structure strengthening the above hypothesis (Figure 4). The same water molecule could also bridge the ligand

Table 2. Experimental and Predicted lnRBA and IC_{50} Values of the Training and Test Sets of Indirubins

ligand	ΔGexp (kcal/mol)	ΔGpred (kcal/mol)	IC_{50}exp (μM)	IC_{50}pred (μM)
		Training Set		
indirubin	−4.605	−5.490	1.000	0.413
indirubin-3′-oxime	−8.422	−7.761	0.022	0.043
5,5′-dibromoindirubin	−5.991	−8.748	0.250	0.016
5-bromoindirubin	−7.505	−6.768	0.055	0.115
5-chloroindirubin	−7.601	−6.829	0.050	0.108
5-fluoroindirubin	−7.156	−6.768	0.078	0.115
5-iodoindirubin-3′-oxime	−9.316	−9.250	0.009	0.010
5-iodoindirubin	−7.293	−6.590	0.068	0.137
5-methylindirubin	−7.386	−7.493	0.062	0.056
5-nitroindirubin	−7.775	−6.930	0.042	0.098
5′-bromoindirubin	−5.655	−6.395	0.350	0.167
6,6′-dibromoindirubin	−3.101	−4.395	4.500	1.234
6,6′-dibromoindirubin-3′-oxime	−6.725	−7.550	0.120	0.053
6-bromoindirubin 6br	−7.706	−7.533	0.045	0.054
6-bromoindirubini-3′-acetoxime	−9.210	−8.181	0.010	0.028
6-bromoindirubin-3′-methoxime	−8.112	−9.369	0.030	0.009
6-bromoindirubin-3′-oxime	−9.903	−8.753	0.005	0.016
6-chloroindirubin	−6.571	−6.844	0.140	0.107
6-chloroindirubin-3′-oxime	−8.517	−8.309	0.020	0.025
6-iodoindirubin	−7.506	−7.801	0.055	0.041
6-iodoindirubin-3′-oxime	−9.210	−8.173	0.010	0.028
6′-bromoindirubin	−1.514	−2.068	22.000	12.644
6′-bromoindirubin-3′-oxime	−5.684	−4.955	0.340	0.705
		Test Set		
5,6-dichloroindirubin	−8.110	−8.850	0.030	0.014
5,6-dichloroindirubin-3′-oxime	−10.120	−9.542	0.004	0.007
6-bromo-5-methylindirubin	−8.290	−10.037	0.025	0.004
6-bromo-5-methylindirubin-3′-oxime	−9.720	−9.981	0.006	0.004
6-bromo-5-nitroindirubin-3′-oxime	−9.560	−9.131	0.007	0.010
6-bromo-5-nitroindirubin	−6.900	−11.186	0.100	0.001
6-fluoroindirubin	−5.030	−6.749	0.650	0.117
6-fluoroindirubin-3′-oxime	−6.640	−7.421	0.130	0.059
6-fluoroindirubin-3′-acetoxime	−7.010	−6.698	0.090	0.123
indirubin-3′-acetoxime	−6.220	−4.199	0.200	1.501
indirubin-3′-methoxime	−6.500	−7.195	0.150	0.075
6-chloroindirubin-3′-acetoxime	−8.680	−7.107	0.017	0.082
5,6-dichloroindirubin-3′-acetoxime	−10.130	−9.102	0.004	0.011
6-bromo-5-methylindirubin-3′-acetoxime	−9.570	−9.632	0.007	0.006
6-bromo-5-nitroindirubin-3′-acetoxime	−9.720	−10.580	0.006	0.003

with the side chain or the backbone carbonyl of $Gln130^{CDK2}$ ($Gln131^{CDK5}$) through the formation of hydrogen bonds. Asp and Gln are conserved in both ATP-binding sites and they are located at approximately the same distance from the water molecule. In GSK-3β this mode of indirect interactions is not completely preserved as a threonine (Thr138) has replaced Asp86. In that case the crystal structure shows clearly that a direct van der Waals contact exists between the γ-CH3 of Thr138 and the indirubin aromatic system. Moreover a possible link between the oxime and the hydroxyl of threonine would need two bridging water molecules (Figure 5). Only one of them is located in the same position as the ribose hydroxyl oxygen in the ATP complex. However, the backbone carbonyl of Gln185 (homologous to $Gln131^{CDK2}$ and $Gln130^{CDK5}$) located at a distance of 3.3 Å from water 47 and the backbone carbonyl of Ile62 placed at a distance of 3.7 Å (Figure 6) from the oxime hydrogen could act as hydrogen bond acceptors of an indirect or direct interaction of the oxime group, respectively.

All the above observations were very important for the interpretation of the biological activity obtained from the synthesized molecules and the understanding of their interaction with their molecular target.

Among the 6-substituted indirubins, the bromo substitution exhibited the highest activity against GSK-3. Calculations showed that this is due mainly to van der Waals interactions which are optimal for both bromo and iodo derivatives in agreement with biological test results.

In previous studies it had been demonstrated that the derivatives substituted on position 5 (especially with the NO_2 group) exhibited an enhanced inhibitory activity.[25] As predicted, combination of the substitutions on both positions 5 and 6 resulted in an additive effect on the activity. The IC_{50} value was reduced about 2 times compared to corresponding single 5-substitution. In agreement with unfavorable steric hindrance between the substituent at C6 and the Phe80 side chain described above, none of the 6- or 5,6- substituted compounds exhibited any substantial inhibitory activity toward CDK1 or CDK5.

Several new 3′-oxime derivatives were synthesized. These compounds exhibited an increased inhibitory activity on all three kinases compared to their nonoxime counterparts, confirming previously reported results. Interesting differences were observed between the inhibitory activities against the three kinases of the 3′-oxime derivatives. The best inhibitory activity on GSK-3 was observed for the 6-bromo- and, more importantly, the 5-,6-disubstituted compounds, reaching low nanomolar IC_{50} values. Compared to the corresponding nonoxime derivatives (Table 1), a 5−10 times increase of inhibitory activity was achieved. According to our theoretical model, this is mainly due to favorable

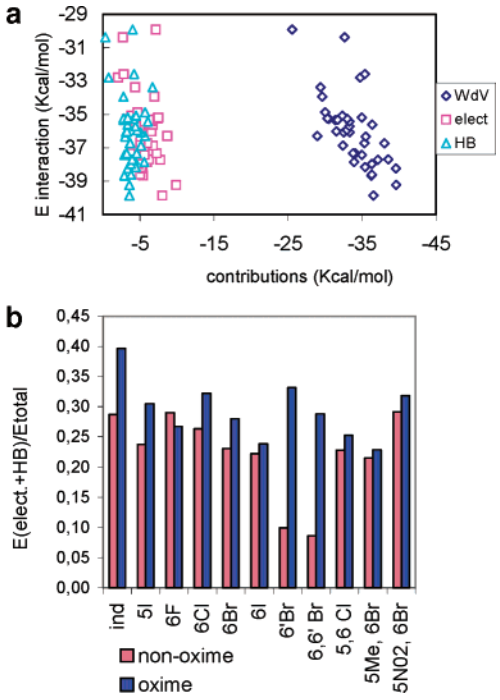

Figure 3. (a) A plot of the values of the three individual energy terms (van der Waals, electrostatic, hydrogen bond) versus the total interaction energy as calculated by PrGen. (b) Comparison of the contribution of the electrostatic and hydrogen bond term expressed by the ratio (elect.+HB)/E_{total} among pairs of oxime and corresponding nonoxime substituted indirubins.

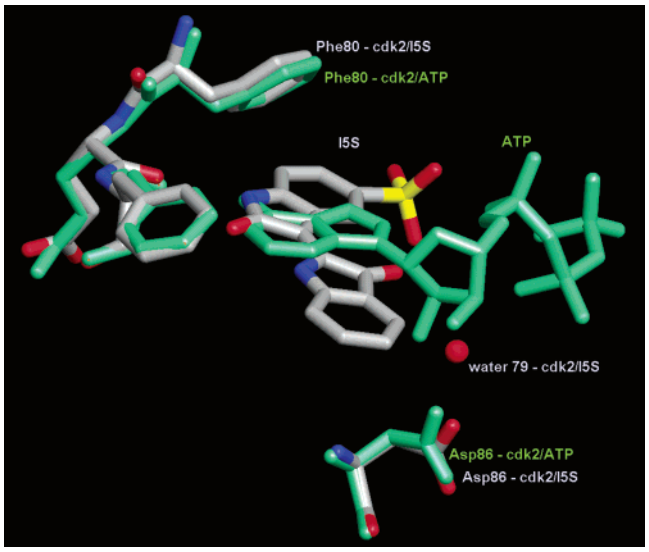

Figure 4. Superimposition of CDK2-I5S and CDK2-ATP. In the cocrystal structure of CDK2-ATP the two hydroxyl groups of the ribose moiety of ATP form hydrogen bonds with the side chain of Asp86. In the structure of CDK2-indirubin 5-sulfonate a water molecule is located approximately at the same position of those hydroxyl groups. This water molecule could bridge the C3′ oxygen with the side chain of Asp86 through the formation of hydrogen bonds, mimicking the interaction formed between the natural substrate and the receptor.

contributions of the electrostatic and hydrogen bond energy, suggesting that the interactions of the oxime hydroxyl group should play an important role in the binding mode stabilization of these structures.

This activity gain was clearly more pronounced with CDK1 and CDK5 although the overall potency was

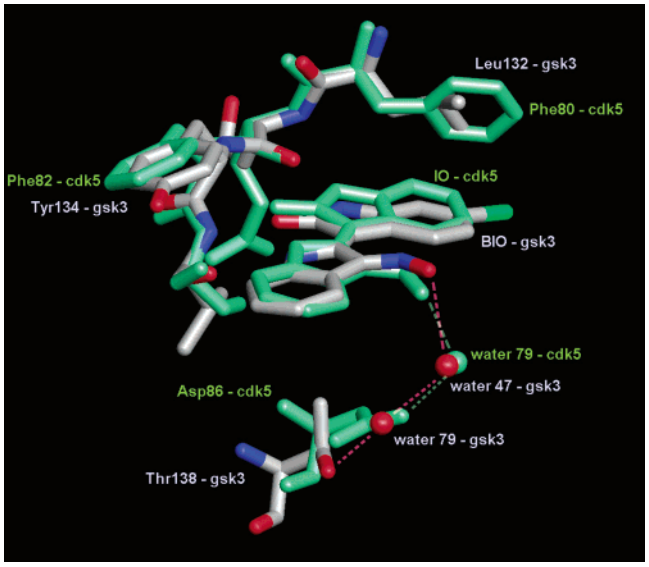

Figure 5. Superimposition of CDK5−IO and GSK-3β-BIO. An indirect interaction of the oxime with the side chain of Asp86 in the CDK5 structure requires one bridging water molecule (water 79). In the GSK-3β structure, Asp86 is replaced by a threonine (Thr138). In this case two bridging water molecules (water 49 and 79) are required to preserve an interaction between the oxime of BIO and the hydroxyl of Thr138.

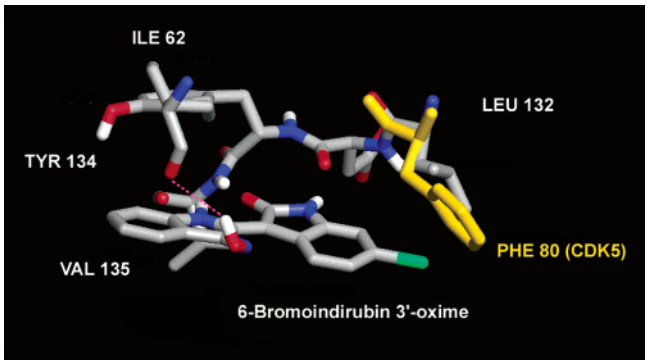

Figure 6. Structure of BIO bound to GSK-3β as resulted from PrGen calculations. The distance between Ile62 carbonyl and the oxime hydrogen is 2.9 Å, suggesting a possible formation of hydrogen bond. In yellow is represented the corresponding position of Phe80 side chain as resulted after superimposition of GSK-3β and CDK5 crystal structure. The steric hindrance between Phe80-CDK5 and the bromine atom of BIO can explain the lower affinity of C6 substituted indirubins for CDK5.

lower than that seen with GSK-3. This inhibitory response should be attributed to the above-mentioned difference between $Asp86^{CDK1-5}$ and the corresponding $Thr138^{GSK-3}$, and the indirect interaction of these amino acid side chains with the 3′-oxime group through one or two water molecules. Moreover, another difference was observed in the 3′-oxime derivatives against CDK1 and CDK5. In all cases these derivatives exhibited a higher activity toward CDK5 than toward CDK1 although the corresponding nonoxime derivatives were equipotent. There are no obvious structural explanations for this phenomenon, but it probably could be attributed to differences in the flexibility of the Gly loop (residues 12−20) as observed in the CDK2 and CDK5 crystal structures. More importantly, the 6-bromo-5-nitro-3′monoxime indirubin derivative (**7g**) displayed an

interesting selectivity for CDK5 compared to CDK1 and this fact should be further explored.

Finally, position 4 was found to be a disadvantageous site for substitution not only because the size of the substituent is a very restricting factor for the chemical synthesis but also because any substituent (as can be observed by molecular modeling) except hydrogen causes a distortion and the molecule loses its planar structure which is necessary for the binding.

Conclusion

Indirubins constitute a promising molecular scaffold from which rather selective molecules active on CDKs, GSK-3, and AhR are starting to be derived. The recent crystallization of several indirubins with CDK2, CDK5, and GSK-3 now provides a solid molecular model allowing one to pinpoint the specific interactions that contribute both to inhibitory efficacy and to kinase selectivity. This model will also be very useful in guiding the synthesis of more pharmacologically friendly indirubins (increased solubility, optimal cell permeability, most favorable tissue, and intracellular distribution), while maintaining potency and selectivity. Like all CDK inhibitors which bind through hydrophobic interactions within the ATP-binding pocket of the enzyme, indirubins are rather hydrophobic. This property constitutes a drawback in the biological use of these compounds, and it is clear that this aspect must be investigated in further work. Increased, but not exaggerated water-solubility is a priority in the development of new indirubins. Of course increased efficiency and increased selectivity remain two major factors to be kept in mind while solubility is optimized.

Finally we plan to make use of this accumulated knowledge to design affinity chromatography media based on indirubins immobilized to beads through an appropriate linkage. These indirubin matrixes will be useful to investigate the real scope of targets of a given indirubin in a given cell type or tissue, as illustrated with other kinase inhibitors.[47] We are also starting to use the detailed understanding of indirubins' interactions with mammalian CDKs and GSK-3 to design indirubins with enhanced specificity for kinases of disease-relevant unicellular parasites such as *Plasmodium falciparum Pf*GSK-3 [48] and *Pf*PK5.[49] Altogether, these studies on indirubins should provide some useful pharmacological tools to investigate the functions of CDKs and GSK-3 in numerous cellular processes (cell division, apoptosis, embryogenesis, etc.). We also hope that they will provide some therapeutically useful compounds against some of the numerous diseases where CDKs or GSK-3 are implicated.

Experimental Section

Chemistry. General Chemistry Experimental Procedures. All chemicals were purchased from Aldrich Chemical Co. NMR spectra were recorded on Bruker DRX 400 and Bruker AC 200 spectrometers [^{1}H (400 and 200 MHz) and ^{13}C (50 MHz)]; chemical shifts are expressed in ppm downfield from TMS. The ^{1}H−^{1}H and the ^{1}H−^{13}C NMR experiments were performed using standard Bruker microprograms. CI-MS spectra were determined on a Finnigan GCQ *Plus* ion-trap mass spectrometer using CH_4 as the CI ionization reagent. Column chromatographies were conducted using flash silica gel 60 Merck (40−63 μm), with an overpressure of 300 mbars. All the compounds gave satisfactory combustion analyses (C, H, N, within ± 0.4% of calculated values).

General Procedure for the Preparation of the Isatins 3a−f. Chloral hydrate (50 g) and Na_2SO_4 (350 g) were dissolved in water (700 mL) in a 3 L beaker and warmed to 35 °C. A warm solution of the appropriate commercial aniline derivative **1a−f** (0.276 mol) in water (200 mL), and an aqueous solution of concentrated HCl (30 mL) was added (a white precipitate of the amine sulfate was formed), followed by a warm solution of hydroxylamine hydrochloride (61 g) in water (275 mL). The mixture was stirred by hand and heated on a hot plate (a thick paste formed at 75−70 °C) at 80−90 °C for 2 h and then allowed to cool for 1 h, by which time the temperature had fallen to 50 °C and filtered. The pale cream product was washed by stirring with water (1 L) and filtered. Drying overnight at 40 °C gave the corresponding isonitrosoacetanilide **2a−f**.

Sulfuric acid (1 L) was heated in a 3 L beaker on a hot plate to 60 °C and then removed. The dry isonitrosoacetanilide **2a−f** was added in portion with stirring over 30 min so that the temperature did not exceed 65 °C. The mixture was then heated to 80 °C for 15 min, allowed to cool to 70 °C, and cooled on ice. The solution was poured on to crushed ice (5 L) and left to stand for 1 h before filtering the orange-red precipitate. The product was washed by stirring with water (400 mL) and filtered to give a mixture of **3a−f** and **4a−f**. The crude product was dissolved in a solution of NaOH (20 g) in water (200 mL) at 60 °C and then acidified with acetic acid (60 mL). After standing 0.5 h and cooling to 35 °C, the **4a−f** precipitate was filtered and washed with water (50 mL). The combined filtrate and washings were acidified with an aqueous concentrated HCl solution (60 mL) and, after standing for 2 h at 5 °C, the **3a−f** precipitate was filtered off and washed with water (50 mL). Yields: **3a**: 27%, **3b**: 14%, **3c**: 29%, **3d**: 22%, **3e**: 33%, **3f**: 31%, **4a**: 56%, **4b**: 64%, **4c**: 53%, **4d**: 59%, **4e**: 49%, **4f**: 51%.

6-Bromo-5-nitroisatin (3g). To a solution of $NaNO_3$ (188 mg, 2.21 mmol) in concentrated H_2SO_4 (3.8 mL) was added dropwise a solution of **3a** (500 mg, 2.21 mmol) in concentrated H_2SO_4 (3.2 mL) for a period of 1 h at 0 °C. The reaction mixture was then poured into ice water (25 mL), and the precipitate was collected by filtration and washed with water to give **3g** (91%).

6-Bromo-*N*-methylisatin (11a). To a solution of **3a** (150 mg, 0.66 mmol) in dry acetone (30 mL) were added Na_2CO_3 (anh.) (1.0 g) and dimethyl sulfate (0.8 mL) under Ar, and the reaction mixture was heated at 60 °C for 20 h. Then, the mixture was filtered, and the filtrate was carefully evaporated using a high vacuum pump (under 40 °C). The solid residue was submitted to flash chromatography with CH_2Cl_2 to afford **11a** (140 mg, 0.58 mmol, 85%)

***N*-Methylisatin (11b).** This compound was prepared from isatin (**3h**) by a procedure analogous to that of **11a**: yield 85%

(2′*Z*)-6-Bromoindirubin (5a). Methanol (18 mL) was vigorously stirred under nitrogen for 20 min and then 6-bromoisatin (**3a**) (100 mg, 0.44 mmol) and 3-acetoxyindole (77 mg, 0.44 mmol) were added, and stirring was continued for 5 min. Anhydrous Na_2CO_3 (114 mg, 1.1 mmol) was added, and the stirring was continued for 3 h. The dark precipitate was filtered and washed with aqueous methanol (1:1, 10 mL) to give **5a** (135 mg, 0.39 mmol, 90%) selectively in a *Z* form. ^{1}H NMR (DMSO, 400 MHz, δ ppm, J in Hz) 11.10 (1H, s, N′-H), 11.00 (1H, s, N−H), 8.67 (1H, d, J = 8.1 Hz, H-4), 7.65 (1H, d, J = 7.5 Hz, H-4′), 7.58 (1H, t, J = 7.5 Hz, H-6′), 7.42 (1H, d, J = 7.5 Hz, H-7′), 7.22 (1H, dd, J = 8.1, 1.7 Hz, H-5), 7.04 (1H, d, J = 1.7 Hz, H-7), 7.03 (1H, t, J = 7.5 Hz, H-5′). ^{13}C NMR (DMSO, 200 MHz, δ ppm) 188.85 (C-3′), 170.98 (C-2), 152.58 (C-7a′), 142.59 (C-7a), 138.86 (C-2′), 137.31 (C-6′), 125.99 (C-4), 124.52 (C-4′), 123.78 (C-5), 121.58 (C-3,5′), 120.86 (C-3a), 119.06 (C-3a′), 113.64 (C-7′), 112.39 (C-7), 105.42 (C-6); CI-MS m/z 341, 343 $(M + H)^+$. Anal. ($C_{16}H_9N_2O_2Br$) C, H, N.

(2′*Z*)-6-Fluoroindirubin (5b). This compound was prepared from 6-fluoroisatin (**3b**) by a procedure analogous to that

of **5a**: yield 75%; ^{1}H NMR (DMSO, 400 MHz, δ ppm, J in Hz) 10.99 (2H, br s, N−H, N′-H), 8.79 (1H, dd, J = 8.7, 6.2 Hz, H-4), 7.65 (1H, d, J = 7.5 Hz, H-4′), 7.58 (1H, t, J = 7.5 Hz, H-6′), 7.41 (1H, d, J = 7.5 Hz, H-7′), 7.02 (1H, t, J = 7.5, Hz, H-5′), 6.83 (1H, td, J = 8.7, 2.5 Hz, H-5), 6.71 (1H, dd, J = 9.1, 2.5 Hz, H-7); CI-MS m/z 281 $(M + H)^+$. Anal. ($C_{16}H_9N_2O_2F$) C, H, N.

(2′*Z*)-6-Iodoindirubin (5c). This compound was prepared from 6-iodoisatin (**3c**) by a procedure analogous to that of **5a**: yield 91%; ^{1}H NMR (DMSO, 400 MHz, δ ppm, J in Hz) 11.04 (1H, s, N′-H), 10.95 (1H, br s, N−H), 8.48 (1H, d, J = 8.5 Hz, H-4), 7.61 (1H, d, J = 7.8 Hz, H-4′), 7.54 (1H, t, J = 7.8 Hz, H-6′), 7.37 (2H, m, H− 5, 7′), 7.19 (1H, s, H-7), 6.99 (1H, t, J = 7.8 Hz, H-5′); CI-MS m/z 389 $(M + H)^+$. Anal. ($C_{16}H_9N_2O_2I$) C, H, N.

(2′*Z*)-6-Chloroindirubin (5d). This compound was prepared from 6-chloroisatin (**3d**) by a procedure analogous to that of **5a**: yield 84%; ^{1}H NMR (DMSO, 400 MHz, δ ppm, J in Hz) 11.07 (1H, s, N′-H), 11.05 (1H, br s, N−H), 8.76 (1H, d, J = 8.5 Hz, H-4), 7.65 (1H, d, J = 7.2 Hz, H-4′), 7.58 (1H, t, J = 7.2 Hz, H-6′), 7.43 (1H, d, J = 7.2 Hz, H-7′), 7.07 (1H, dd, J = 8.5, 1.7 Hz, H-5), 7.03 (1H, t, J = 7.2 Hz, H-5′), 6.91 (1H, t, J = 1.7 Hz, H-7); CI-MS m/z 297, 299 $(M + H)^+$. Anal. ($C_{16}H_9N_2O_2Cl$) C, H, N.

(2′*Z*)-5,6-Dichloroindirubin (5e). This compound was prepared from 5,6-dichloroisatin (**3e**) by a procedure analogous to that of **5a**: yield 77%; ^{1}H NMR (DMSO, 400 MHz, δ ppm, J in Hz) 11.17 (2H, s, N−H, N′-H) 8.94 (1H, s, H-4), 7.67 (1H, d, J = 7.5 Hz, H-4′), 7.60 (1H, t, J = 7.5 Hz, H-6′), 7.43 (1H, d, J = 7.5, Hz, H-7′), 7.08 (1H, s, H-7), 7.06 (1H, t, J = 7.5 Hz, H-5′); CI-MS m/z 331, 333, 335 $(M + H)^+$. Anal. ($C_{16}H_8N_2O_2Cl_2$) C, H, N.

(2′*Z*)-6-Bromo-5-methylindirubin (5f). This compound was prepared from 6-bromo-5-methylisatin (**3f**) by a procedure analogous to that of **5a**: yield 76%; ^{1}H NMR (DMSO, 400 MHz, δ ppm, J in Hz) 11.06 (1H, s, N′-H), 10.94 (1H, br s, N−H) 8.73 (1H, s, H-4), 7.65 (1H, d, J = 7.5 Hz, H-4′), 7.58 (1H, t, J = 7.5 Hz, H-6′), 7.42 (1H, d, J = 7.5, Hz, H-7′), 7.06 (1H, s, H-7), 7.03 (1H, t, J = 7.5 Hz, H-5′), 2.36 (3H, s, 5-CH_3); CI-MS m/z 355, 357 $(M + H)^+$. Anal. ($C_{17}H_{11}N_2O_2Br$) C, H, N.

(2′*Z*)-6-Bromo-5-nitroindirubin (5g). This compound was prepared from 6-bromo-5-nitroisatin (**3g**) by a procedure analogous to that of **5a**: yield 41%; ^{1}H NMR (DMSO, 400 MHz, δ ppm, J in Hz) 11.57 (1H, br s, N′-H), 11.31 (1H, s, N−H) 9.46 (1H, s, H-4), 7.70 (1H, d, J = 7.5 Hz, H-4′), 7.62 (1H, t, J = 7.5 Hz, H-6′), 7.45 (1H, d, J = 7.5, Hz, H-7′), 7.26 (1H, s, H-7), 7.08 (1H, t, J = 7.5 Hz, H-5′); CI-MS m/z 386, 388 $(M + H)^+$. Anal. ($C_{16}H_8N_3O_4Br$) C, H, N.

(2′*Z*)-6-Vinylindirubin (5i). To a solution of 6-bromoindirubin (**5a**) (250 mg, 0.73 mmol) in dioxane (5 mL) were added tetrakis(triphenylphosphine)palladium (18 mg) and tributylvinylstanate (0.32 mL, 1.1 mmol), and the reaction mixture was heated at 100 °C for 1 h. Then the solvent was evaporated under reduced pressure and the residue was washed with cyclohexane and recrystallized from methanol to give **5i** (160 mg, 76%); ^{1}H NMR (DMSO, 400 MHz, δ ppm, J in Hz) 11.02 (2H, s, N−H, N′-H), 8.74 (1H, d, J = 7.9 Hz, H-4), 7.65 (1H, d, J = 7.5 Hz, H-4′), 7.57 (1H, t, J = 7.5 Hz, H-6′), 7.42 (1H, d, J = 7.5 Hz H-7′), 7.15 (1H, dd, J = 7.9, 1.7 Hz, H-5) 7.02 (1H, t, J = 7.5 Hz H-5′), 6.99 (1H, d, J = 1.7 Hz, H-7) 6.76 (1H, dd, J = 17.4, 10.8 Hz, H-1″) 5.85 (1H, d, J = 17.4 Hz, H-2b″) 5.30 (1H, d, J = 10.8 Hz, H-2a″); CI-MS m/z 289 $(M + H)^+$. Anal. ($C_{18}H_{12}N_2O_2$) C, H, N.

(2′*Z*)-4-Chloroindirubin (6). This compound was prepared from 4-chloroisatin (**4d**) by a procedure analogous to that of **5a**: yield 5%; ^{1}H NMR (DMSO, 400 MHz, δ ppm, J in Hz) 11.24 (1H, br s, N′-H), 10.95 (1H, br s, N−H), 7.64 (1H, d, J = 7.2 Hz, H-4′), 7.56 (1H, t, J = 7.2 Hz, H-6′), 7.35 (1H, d, J = 7.2 Hz, H-7′), 7.19 (1H, t, J = 7.5 Hz, H-6), 7.03 (1H, t, J = 7.2 Hz, H-5′), 7.00 (1H, d, J = 7.5 Hz, H-5), 6.83 (1H, d, J = 7.5 Hz, H-7); CI-MS m/z 297, 299 $(M + H)^+$. Anal. ($C_{16}H_9N_2O_2Cl$) C, H, N.

(2′*Z*)-6′-Bromoindirubin (12a). This compound was prepared from isatin (**3h**) and 6-bromo-3-acetoxyindole (**10a**) by a procedure analogous to that of **5a**: yield 80%; ^{1}H NMR (DMSO, 400 MHz, δ ppm, J in Hz) 11.00 (1H, s, N′-H), 10.90 (1H, s, N−H), 8.75 (1H, d, J = 7.7 Hz, H-4), 7.64 (1H, s, H-7′), 7.59 (1H, d, J = 8.1 Hz, H-4′), 7.27 (1H, t, J = 7.7 Hz, H-6), 7.19 (1H, d, J = 8.1 Hz, H-5′), 7.03 (1H, t, J = 7.7 Hz, H-5), 6.92 (1H, d, J = 7.7 Hz, H-7). ^{13}C NMR (DMSO, 200 MHz, δ ppm) 187.17 (C-3′), 170.33 (C-2), 152.76 (C-7a′), 140.71 (C-7a), 137.58 (C-2′), 130.34 (C-6′), 129.28 (C-6), 125.45 (C-4′), 124.46 (C-4), 123.65 (C-5′), 120.93 (C-5, 3a), 117.77 (C-3a′), 115.82 (C-7′), 109.24 (C-7), 107.26 (C-3); CI-MS m/z 341, 343 $(M + H)^+$. Anal. ($C_{16}H_9N_2O_2Br$) C, H, N.

(2′*Z*)-6,6′-Dibromoindirubin (12b). This compound was prepared from 6-bromoisatin (**3a**) and 6-bromo-3-acetoxyindole (**10a**) by a procedure analogous to that of **5a**: yield 76%; ^{1}H NMR (DMSO, 400 MHz, δ ppm, J in Hz) 11.20 (1H, s, N′-H), 11.10 (1H, s, N−H), 8.67 (1H, d, J = 8.4 Hz, H-4), 7.68 (1H, d, J = 1.7 Hz H-7′), 7.62 (1H, d, J = 8.1 Hz, H-4′), 7.22 (1H, dd, J = 8.1, 1.7 Hz, H-5′), 7.22 (1H, dd, J = 8.4, 1.6 Hz, H-5), 7.05 (1H, d, J = 1.6 Hz, H-7). ^{13}C NMR (DMSO, 200 MHz, δ ppm) 187.60 (C-3′), 170.69 (C-2), 153.04 (C-7a′), 142.49 (C-7a), 130.99 (C-6′), 129.55 (C-2′), 126.25 (C-4), 126.06 (C-4′), 124.45 (C-5′), 124.08 (C-5), 121.95 (C-3), 121.04 (C-3a), 118.31 (C-3a′), 116.47 (C-7′), 112.50 (C-7), 106.01 (C-6); CI-MS m/z 419, 421, 423 $(M + H)^+$. Anal. ($C_{16}H_8N_2O_2Br_2$) C, H, N.

(2′*Z*)-6-Bromo-1-methylindirubin (12c). This compound was prepared from 6-bromo-*N*-methylisatin (**11a**) and 3-acetoxyindole (**10b**) by a procedure analogous to that of **5a**: yield 49%; ^{1}H NMR (DMSO, 400 MHz, δ ppm, J in Hz) 11.13 (1H, s, N′-H), 8.70 (1H, d, J = 8.2 Hz, H-4), 7.66 (1H, d, J = 7.8 Hz, H-4′), 7.60 (1H, t, J = 7.8 Hz, H-6′), 7.43 (1H, d, J = 7.8, Hz, H-7′), 7.35 (1H, d, J = 1 Hz, H-7), 7.29 (1H, dd, J = 8.2, 1 Hz, H-5), 7.04 (1H, t, J = 7.8, Hz, H-5′), 3.28 (3H, s, N−CH_3); CI-MS m/z 355, 357 $(M + H)^+$. Anal. ($C_{17}H_{11}N_2O_2Br$) C, H, N.

(2′*Z*)-1-Methylindirubin (12d). This compound was prepared from *N*-methylisatin (**11b**) and 3-acetoxyindole (**10b**) by a procedure analogous to that of **5a**: yield 44%; ^{1}H NMR (DMSO, 400 MHz, δ ppm, J in Hz) 11.07 (1H, s, N′-H), 8.80 (1H, d, J = 7.5 Hz, H-4), 7.66 (1H, d, J = 7.5 Hz, H-4′), 7.59 (1H, t, J = 7.5 Hz, H-6′), 7.42 (1H, d, J = 7.5 Hz, H-7′), 7.35 (1H, t, J = 7.5 Hz, H-6), 7.10 (1H, t, J = 7.5 Hz, H-5), 7.08 (1H, d, J = 7.5 Hz, H-7), 7.03 (1H, t, J = 7.5 Hz, H-5′), 3.28 (3H, s, N−CH_3); CI-MS m/z 277 $(M + H)^+$. Anal. ($C_{17}H_{12}N_2O_2$) C, H, N.

General Procedure for the Preparation of the Oximes 7a−i and 13a−d. The appropriate indirubin derivative **5a−i** and **12a−d** (1 mmol) was dissolved in pyridine (10 mL). With magnetic stirring, hydroxylamine hydrochloride (10 equiv) was added and the mixture was heated under reflux (120 °C) for 1.5 h. Then the solvent was evaporated under reduced pressure, and the residue was washed with water and cyclohexane to afford quantitatively the corresponding 3′-oxime selectively in a (2′*Z*,3′*E*) form.

Data for (2′*Z*,3′*E*)-6-Bromoindirubin-3′-oxime (7a). ^{1}H NMR (DMSO, 400 MHz, δ ppm, J in Hz) 13.61 (1H, br s, NOH), 11.72 (1H, s, N′-H), 10.85 (1H, s, N−H), 8.53 (1H, d, J = 8.2 Hz, H-4), 8.19 (1H, d, J = 7.5 Hz, H-4′), 7.39 (2H, br s, H-6′, 7′), 7.07 (1H, d, J = 8.2, Hz, H-5), 7.01 (2H, br s, H-7, 5′); CI-MS m/z 356, 358 $(M + H)^+$. Anal. ($C_{16}H_{10}N_3O_2Br$) C, H, N.

Data for (2′*Z*,3′*E*)-6-Fluoroindirubin-3′-oxime (7b). ^{1}H NMR (DMSO, 400 MHz, δ ppm, J in Hz) 13.52 (1H, s, NOH), 11.65 (1H, s, N−H), 10.86 (1H, s, N′-H) 8.65 (1H, dd, J = 8.8, 5.9 Hz, H-4), 8.23 (1H, d, J = 7.3 Hz, H-4′), 7.40 (2H, m, H-6′, 7′), 7.02 (1H, m, H-5′), 6.75 (1H, td, J = 8.8, 2.4 Hz, H-5), 6.70 (1H, dd, J = 8.8, 2.4 Hz, H-7); CI-MS m/z 296 $(M + H)^+$. Anal. ($C_{16}H_{10}N_3O_2F$) C, H, N.

Data for (2′*Z*,3′*E*)-6-Iodoindirubin-3′-oxime (7c). ^{1}H NMR (acetone, 400 MHz, δ ppm, J in Hz) 13.20 (1H, s, NOH), 11.70 (1H, s, N′-H), 9.98 (1H, s, N−H), 8.43 (1H, d, J = 8.3 Hz, H-4), 8.28 (1H, d, J = 7.5 Hz, H-4′), 7.39 (1H, t, J = 7.5 Hz, H-6′), 7.30 (1H, d, J = 7.5, Hz, H-7′), 7.28 (1H, d, J = 1.3 Hz H-7) 7.23 (1H, dd, J = 8.3, 1.3 Hz, H-5) 7.03 (1H, t, J = 7.5 Hz, H-5′); CI-MS m/z 404 $(M + H)^+$. Anal. ($C_{16}H_{10}N_3O_2I$) C, H, N.

Data for (2′*Z*,3′*E*)-6-Chloroindirubin-3′-oxime (7d). ^{1}H NMR (acetone, 400 MHz, δ ppm, J in Hz) 13.60 (1H, s, NOH), 11.76 (1H, s, N′-H), 10.10 (1H, s, N−H), 8.71 (1H, d, J = 8.8 Hz, H-4), 8.37 (1H, d, J = 7.5 Hz, H-4′), 7.48 (1H, t, J = 7.5 Hz, H-6′), 7.38 (1H, d, J = 7.5 Hz, H-7′) 7.12 (1H, t, J = 7.5 Hz, H-5′), 7.04 (1H, d, J = 2.2 Hz, H-7) 7.12 (1H, dd, J = 8.8, 2.2 Hz, H-5); CI-MS m/z 312, 314 $(M + H)^+$. Anal. ($C_{16}H_{10}N_3O_2$-Cl) C, H, N.

Data for (2′*Z*,3′*E*)-5,6-Dichloroindirubin-3′-oxime (7e). ^{1}H NMR (DMSO, 400 MHz, δ ppm, J in Hz) 13.76 (1H, br s, NOH), 11.88 (1H, s, N′-H), 10.90 (1H, s, N−H), 8.80 (1H, s, H-4), 8.25 (1H, d, J = 7.5 Hz, H-4′), 7.44 (1H, d, J = 7.9 Hz, H-7′), 7.39 (1H, t, J = 7.9 Hz, H-6′) 7.06 (1H, t, J = 7.9 Hz, H-5′) 7.03 (1H, s, H-7); CI-MS m/z 346, 348, 350 $(M + H)^+$. Anal. ($C_{16}H_9N_3O_2Cl_2$) C, H, N.

Data for (2′*Z*,3′*E*)-6-Bromo-5-methylindirubin-3′-oxime (7f). ^{1}H NMR (DMSO, 400 MHz, δ ppm, J in Hz) 13.56 (1H, br s, NOH), 11.74 (1H, s, N′-H), 10.69 (1H, s, N−H), 8.62 (1H, s, H-4), 8.22 (1H, d, J = 7.9 Hz, H-4′), 7.39 (2H, m, H-6′, 7′), 7.03 (1H, s, H-7), 7.04 (1H, dd, J = 8.1, 2.1 Hz, H-5′), 2.37 (3H, s, 5-CH_3); CI-MS m/z 370, 372 $(M + H)^+$. Anal. ($C_{17}H_{12}N_3O_2$-Br) C, H, N.

Data for (2′*Z*,3′*E*)-6-Bromo-5-nitroindirubin-3′-oxime (7g). ^{1}H NMR (DMSO, 400 MHz, δ ppm, J in Hz) 13.90 (1H, br s, NOH), 11.91 (1H, s, N′-H), 11.33 (1H, s, N−H), 9.20 (1H, s, H-4), 8.24 (1H, d, J = 7.5 Hz, H-4′), 7.50 (1H, d, J = 7.5 Hz, H-7′), 7.43 (1H, t, J = 7.5 Hz, H-6′) 7.23 (1H, s, H-7), 7.10 (1H, t, J = 7.5 Hz, H-5′); CI-MS m/z 401, 403 $(M + H)^+$. Anal. ($C_{16}H_9N_4O_4Br$) C, H, N.

Data for (2′*Z*,3′*E*)-6-Vinylindirubin-3′-oxime (7i). ^{1}H NMR (DMSO, 400 MHz, δ ppm, J in Hz) 13.57 (1H, br s, NOH), 11.72 (1H, s, N′-H), 10.76 (1H, s, N−H), 8.60 (1H, d, J = 8.3 Hz, H-4), 8.23 (1H, d, J = 7.3 Hz, H-4′), 7.41 (2H, m, H-6′, 7′), 7.03 (3H, m, H-5, 5′, 7), 6.74 (1H, dd, J = 17.6, 10.8 Hz, H-1″) 5.77 (1H, d, J = 17.6 Hz, H-2b″) 5.22 (1H, d, J = 10.8 Hz, H-2a″); CI-MS m/z 304 $(M + H)^+$. Anal. ($C_{18}H_{13}N_3O_2$) C, H, N.

Data for (2′*Z*,3′*E*)-6′-Bromo-indirubin-3′-oxime (12a). ^{1}H NMR (DMSO, 400 MHz, δ ppm, J in Hz) 13.75 (1H, br s, NOH), 11.70 (1H, s, N′-H), 10.72 (1H, s, N−H), 8.61 (1H, d, J = 7.9 Hz, H-4), 8.12 (1H, d, J = 8.3 Hz, H-4′), 7.63 (1H, d, J = 1.2 Hz, H-7′), 7.19 (1H, dd, J = 1.2, 8.3 Hz, H-5′), 7.14 (1H, d, J = 7.9 Hz, H-6), 6.95 (1H, t, J = 7.9 Hz, H-5), 6.91 (1H, d, J = 7.9 Hz, H-7); CI-MS m/z 356, 358 $(M + H)^+$. Anal. ($C_{16}H_{10}N_3O_2Br$) C, H, N.

Data for (2′*Z*,3′*E*)-6,6′-Dibromo-indirubin-3′-oxime (12b). ^{1}H NMR (DMSO, 400 MHz, δ ppm, J in Hz) 13.84 (1H, br s, NOH), 11.70 (1H, s, N′-H), 10.85 (1H, s, N−H), 8.51 (1H, d, J = 8.7 Hz, H-4), 8.10 (1H, d, J = 8.3 Hz, H-4′), 7.63 (1H, s, H-7′), 7.20 (1H, d, J = 8.3 Hz, H-5′), 7.08 (1H, d, J = 8.7 Hz, H-5), 7.06 (1H, s, H-7); CI-MS m/z 434, 436,438 $(M + H)^+$. Anal. ($C_{16}H_9N_3O_2Br_2$) C, H, N.

Data for (2′*Z*,3′*E*)-6-Bromo-1-methylindirubin-3′-oxime (12c). ^{1}H NMR (DMSO, 400 MHz, δ ppm, J in Hz) 13.69 (1H, br s, NOH), 11.78 (1H, s, N′-H), 8.61 (1H, d, J = 8.1 Hz, H-4), 8.23 (1H, d, J = 7.3 Hz, H-4′), 7.44 (2H, m, H-6′, 7′), 7.31 (1H, s, H-7), 7.17 (1H, d, J = 8.1 Hz, H-5), 7.07 (1H, br s, H-5′), 3.32 (3H, s, N−CH_3); CI-MS m/z 370, 372 $(M + H)^+$. Anal. ($C_{17}H_{12}N_3O_2Br$) C, H, N.

Data for (2′*Z*,3′*E*)-1-Methylindirubin-3′-oxime (12d). ^{1}H NMR (DMSO, 400 MHz, δ ppm, J in Hz) 13.56 (1H, br s, NOH), 11.74 (1H, s, N′-H), 8.69 (1H, d, J = 7.8 Hz, H-4), 8.23 (1H, d, J = 7.5 Hz, H-4′), 7.41 (2H, m, H-6′, 7′), 7.23 (1H, t, J = 7.8, Hz, H-6), 7.04 (3H, m, H-5′, 5, 7), 3.31 (3H, s, N−CH_3); CI-MS m/z 292 $(M + H)^+$. Anal. ($C_{17}H_{13}N_3O_2$) C, H, N.

General Procedure for the Preparation of the Acetoximes 8a−i and 14. The appropriate indirubin-3′-oxime derivative **7a−i** and **13c** (0.2 mmol) was dissolved in pyridine (10 mL). Ac_2O was added (0.5 mL), and the mixture was stirred for 30 min at 0 °C. Then water (1 mL) was added, and the solvents were evaporated under reduced pressure. The residue was washed with water and cyclohexane to afford quantitatively the corresponding 3′-acetoxime selectively in a (2′*Z*,3′*E*) form.

Data for (2′*Z*,3′*E*)-6-Bromoindirubin-3′-acetoxime (8a). ^{1}H NMR (DMSO, 400 MHz, δ ppm, J in Hz) 11.60 (1H, s, N′-H), 11.01 (1H, s, N−H), 9.02 (1H, d, J = 8.5 Hz, H-4), 8.24 (1H, d, J = 7.8, H-4′), 7.52 (1H, d, J = 7.8, H-7′), 7.49 (1H, t, J = 7.8 Hz, H-6′), 7.10 (1H, t, J = 7.8 Hz, H-5′), 7.09 (1H, d, J = 8.5 Hz, H-5), 7.04 (1H, s, H-7), 2.47 (3H, s, OCOCH_3); CI-MS m/z 397, 399 $(M + H)^+$. Anal. ($C_{18}H_{12}N_3O_3Br$) C, H, N.

Data for (2′*Z*,3′*E*)-6-Fluoroindirubin-3′-acetoxime (8b). ^{1}H NMR (DMSO, 400 MHz, δ ppm, J in Hz) 11.50 (1H, s, N′-H), 11.03 (1H, s, N−H), 9.12 (1H, dd, J = 8.7, 5.8 Hz, H-4), 8.25 (1H, d, J = 7.5, H-4′), 7.52 (1H, t, J = 7.5, H-6′), 7.46 (1H, d, J = 7.5 Hz, H-7′), 7.08 (1H, t, J = 7.5 Hz, H-5′), 6.73 (2H, m, H− 5, 7), 2.46 (3H, s, OCOCH_3); CI-MS m/z 338 $(M + H)^+$. Anal. ($C_{18}H_{12}N_3O_3F$) C, H, N.

Data for (2′*Z*,3′*E*)-6-Iodoindirubin-3′-acetoxime (8c). ^{1}H NMR (DMSO, 400 MHz, δ ppm, J in Hz) 11.57 (1H, s, N′-H), 10.92 (1H, s, N−H), 8.83 (1H, d, J = 8.3 Hz, H-4), 8.21 (1H, d, J = 7.9, H-4′), 7.50 (1H, d, J = 7.9, H-7′), 7.45 (1H, t, J = 7.9 Hz, H-6′), 7.25 (1H, d, J = 8.3 Hz, H-5), 7.18 (1H, s, H-7), 7.06 (1H, t, J = 7.9 Hz, H-5′), 2.47 (3H, s, OCOCH_3); CI-MS m/z 446 $(M + H)^+$. Anal. ($C_{18}H_{12}N_3O_3I$) C, H, N.

Data for (2′*Z*,3′*E*)-6-Chloroindirubin-3′-acetoxime (8d). ^{1}H NMR (DMSO, 400 MHz, d ppm, J in Hz) 11.59 (1H, s, N′-H), 11.02 (1H, s, N−H), 9.09 (1H, d, J = 8.2 Hz, H-4), 8.25 (1H, d, J = 7.8 Hz, H-4′), 7.50 (2H, m, H-6′, 7′), 7.10 (1H, t, J = 7.8 Hz, H-5′), 6.96 (1H, dd, J = 2.3, 8.2 Hz, H-5), 6.91 (1H, d, J = 2.3 Hz, H-7), 2.47 (3H, s, OCOCH_3); CI-MS m/z 354, 356 $(M + H)^+$. Anal. ($C_{18}H_{12}N_3O_3Cl$) C, H, N.

Data for (2′*Z*,3′*E*)-5,6-Dichloroindirubin-3′-acetoxime (8e). ^{1}H NMR (DMSO, 400 MHz, δ ppm, J in Hz) 11.65 (1H, s, N′-H), 11.08 (1H, s, N−H), 9.33 (1H, s, H-4), 8.24 (1H, d, J = 7.4 Hz, H-4′), 7.52 (2H, m, H-6′, 7′), 7.12 (1H, t, J = 7.4 Hz, H-5′) 7.04 (1H, s, H-7) 2.48 (3H, s, OCOCH_3); CI-MS m/z 388, 390, 392 $(M + H)^+$. Anal. ($C_{18}H_{11}N_3O_3Cl_2$) C, H, N.

Data for (2′*Z*,3′*E*)-6-Bromo-5-methylindirubin-3′-acetoxime (8f). ^{1}H NMR (DMSO, 400 MHz, δ ppm, J in Hz) 11.56 (1H, s, N′-H), 10.87 (1H, s, N−H), 9.16 (1H, s, H-4), 8.26 (1H, d, J = 7.8 Hz, H-4′), 7.50 (2H, m, H-6′, 7′), 7.10 (1H, t, J = 7.8 Hz, H-5′), 7.05 (1H, s, H-7), 2.48 (3H, s, OCOCH_3), 2.39 (3H, s, 5-CH_3); CI-MS m/z 412, 414 $(M + H)^+$. Anal. ($C_{19}H_{14}N_3O_3$-Br) C, H, N.

Data for (2′*Z*,3′*E*)-6-Bromo-5-nitroindirubin-3′-acetoxime (8g). ^{1}H NMR (DMSO, 400 MHz, δ ppm, J in Hz) 11.73 (1H, s, N′-H), 11.41 (1H, s, N−H), 9.56 (1H, s, H-4), 8.22 (1H, d, J = 7.8 Hz, H-4′), 7.53 (2H, m, H-6′, 7′), 7.21 (1H, s, H-7), 7.13 (1H, t, J = 7.8 Hz, H-5′) 2.46 (3H, s, OCOCH_3); CI-MS m/z 443, 445 $(M + H)^+$. Anal. ($C_{18}H_{11}N_4O_5Br$) C, H, N.

Data for (2′*Z*,3′*E*)-Indirubin-3′-acetoxime (8h). ^{1}H NMR (DMSO, 400 MHz, δ ppm, J in Hz) 11.59 (1H, s, N′-H), 10.87 (1H, s, N−H), 9.08 (1H, d, J = 7.8 Hz, H-4), 8.26 (1H, d, J = 7.8 Hz, H-4′), 7.52 (1H, t, J = 7.8 Hz, H-6′), 7.46 (1H, t, J = 7.8 Hz, H-7′) 7.20 (1H, t, J = 7.8 Hz, H-6), 7.08 (1H, t, J = 7.8 Hz, H-5), 6.97 (1H, t, J = 7.8 Hz, H-5′), 6.90 (1H, d, J = 7.8 Hz, H-7), 2.47 (3H, s, OCOCH_3); CI-MS m/z 320 $(M + H)^+$. Anal. ($C_{18}H_{13}N_3O_3$) C, H, N.

Data for (2′*Z*,3′*E*)-6-Vinylindirubin-3′-acetoxime (8i). ^{1}H NMR (DMSO, 400 MHz, δ ppm, J in Hz) 11.57 (1H, s, N′-H), 10.90 (1H, s, N−H), 9.05 (1H, d, J = 8.2 Hz, H-4), 8.25 (1H, d, J = 7.4 Hz, H-4′), 7.49 (2H, m, H-6′, 7′), 7.08 (2H, m, H-5, 5′) 6.99 (1H, s, H-7), 6.76 (1H, dd, J = 17.6, 11.3 Hz, H-1″), 5.81 (1H, d, J = 17.6 Hz, H-2b″), 5.25 (1H, d, J = 10.9 Hz, H-2a″), 2.47 (3H, s, OCOCH_3); CI-MS m/z 346 $(M + H)^+$. Anal. ($C_{20}H_{15}N_3O_3$) C, H, N.

Data for (2′*Z*,3′*E*)-6-Bromo-1-methylindirubin-3′-acetoxime (14). ^{1}H NMR (DMSO, 400 MHz, δ ppm, J in Hz) 11.63 (1H, s, N′-H), 9.06 (1H, d, J = 8.3 Hz, H-4), 8.25 (1H, d, J = 7.4 Hz, H-4′), 7.51 (2H, m, H-6′, 7′), 7.34 (1H, d, J = 1.7 Hz, H-7), 7.16 (1H, dd, J = 1.7, 8.3 Hz, H-5), 7.11 (1H, t, J = 7.4 Hz, H-5′), 3.31 (3H, s, N−CH_3), 2.48 (3H, s, OCOCH_3); CI-MS m/z 412, 414 $(M + H)^+$. Anal. ($C_{19}H_{14}N_3O_3Br$) C, H, N.

(2′*Z*,3′*E*)-6-Bromoindirubin-3′-methoxime (9a). To a solution of 6-bromoindirubin (**5a**) (26 mg, 0.076 mmol) in pyridine (2 mL) was added methoxylamine hydrochloride (30 mg), and the mixture was heated under reflux (120 °C) for 12

h. Then the solvent was evaporated under reduced pressure, and the residue was washed with water and diethyl ether to afford **9** (16 mg, 0.043 mmol, 57% selectively in a (2′*Z*,3′*E*) form. ^{1}H NMR (DMSO, 400 MHz, δ ppm, *J* in Hz) 11.70 (1H, s, N′-H), 10.92 (1H, s, N−H), 8.54 (1H, d, $J = 8.5$ Hz, H-4), 8.11 (1H, d, $J = 7.8$, H-4′), 7.43 (2H, br s, H-6′, 7′), 7.17 (1H, d, $J = 8.5$ Hz, H-5), 7.04 (2H, br s, H-7, 5′), 4.39 (3H, s, OCH_3); CI-MS *m*/*z* 371, 369 $(M + H)^+$. Anal. ($C_{17}H_{12}N_3O_2Br$) C, H, N.

(2′*Z*,3′*E*)-Indirubin-3′-methoxime (9b). This compound was prepared from indirubin (**5h**) by a procedure analogous to that of **9a**: yield 63%;^{1}H NMR (DMSO, 400 MHz, δ ppm, *J* in Hz) 11.69 (1H, s, N′-H), 10.78 (1H, s, N−H), 8.63 (1H, d, *J* = 7.8 Hz, H-4), 8.12 (1H, d, $J = 7.4$ Hz, H-4′), 7.43 (2H, m, H-6′, 7′), 7.16 (1H, t, $J = 7.8$, Hz, H-6), 7.01 (2H, m, H-5, 5′), 6.90 (2H, d, $J = 7.8$ Hz, H-7), 4.38 (3H, s, OCH_3); CI-MS *m*/*z* 292 $(M + H)^+$. Anal. ($C_{17}H_{13}N_3O_2$) C, H, N.

Biochemistry. Biochemical Reagents. Sodium orthovanadate, EGTA, EDTA, Mops, β-glycerophosphate, phenyl phosphate, sodium fluoride, dithiothreitol (DTT), glutathione-agarose, glutathione, bovine serum albumin (BSA), nitrophenyl phosphate, leupeptin, aprotinin, pepstatin, soybean trypsin inhibitor, benzamidine, and histone H1 (type III−S) were obtained from Sigma Chemicals. [γ-^{33}P]-ATP was obtained from Amersham. The GS-1 peptide (YRRAAVPPSPSLSRHS-SPHQSpEDEEE) was synthesized by the Peptide Synthesis Unit, Institute of Biomolecular Sciences, University of Southampton, Southampton SO16 7PX, U.K.

Buffers. 1. Homogenization Buffer: 60 mM β-glycerophosphate, 15 mM *p*-nitrophenyl phosphate, 25 mM Mops (pH 7.2), 15 mM EGTA, 15 mM $MgCl_2$, 1 mM DTT, 1 mM sodium vanadate, 1 mM NaF, 1 mM phenyl phosphate, 10 μg leupeptin/mL, 10 μg aprotinin/mL, 10 μg soybean trypsin inhibitor/mL, and 100 μM benzamidine.

2. Buffer A: 10 mM $MgCl_2$, 1 mM EGTA, 1 mM DTT, 25 mM Tris-HCl pH 7.5, 50 μg heparin/mL.

3. Buffer C: homogenization buffer but 5 mM EGTA, no NaF and no protease inhibitors.

Kinase Preparations and Assays. Kinases activities were assayed in Buffer A or C (unless otherwise stated), at 30 °C, at a final ATP concentration of 15 μM. Blank values were subtracted and activities calculated as pmoles of phosphate incorporated for a 10 min incubation. The activities were expressed in % of the maximal activity, i.e., in the absence of inhibitors. Controls were performed with appropriate dilutions of dimethyl sulfoxide.

GSK-3α/β was purified from porcine brain by affinity chromatography on immobilized axin.[50] It was assayed, following a 1/100 dilution in 1 mg BSA/mL 10 mM DTT, with 5 μL 40 μM GS-1 peptide as a substrate, in buffer A, in the presence of 15 μM [γ-^{33}P] ATP (3000 Ci/mmol; 1 mCi/mL) in a final volume of 30 μL. After 30 min incubation at 30 °C, 25 μL aliquots of supernatant were spotted onto 2.5 × 3 cm pieces of Whatman P81 phosphocellulose paper, and, 20 s later, the filters were washed five times (for at least 5 min each time) in a solution of 10 mL phosphoric acid/liter of water. The wet filters were counted in the presence of 1 mL of ACS (Amersham) scintillation fluid.

CDK1/cyclin B was extracted in homogenization buffer from M phase starfish (*Marthasterias glacialis*) oocytes and purified by affinity chromatography on p9^{CKShs1}-sepharose beads, from which it was eluted by free p9^{CKShs1} as previously described.[51] The kinase activity was assayed in buffer C, with 1 mg histone H1 /mL, in the presence of 15 μM [γ-^{32}P] ATP (3000 Ci/mmol; 1 mCi/mL) in a final volume of 30 μL. After 10 min incubation at 30 °C, 25 μL aliquots of supernatant were spotted onto P81 phosphocellulose papers and treated as described above.

CDK5/p25 was reconstituted by mixing equal amounts of recombinant mammalian CDK5 and p25 expressed in *E. coli* as GST (Glutathione-S-transferase) fusion proteins and purified by affinity chromatography on glutathione-agarose (vectors kindly provided by Dr. J. H. Wang) (p25 is a truncated version of p35, the 35 kDa CDK5 activator). Its activity was assayed in buffer C as described for CDK1/cyclin B.

Molecular Modeling. The 38 ligand molecules (training and test set) were designed and energy-minimized (AMBER*) using MACROMODEL software.[52] Partial atomic charges were attributed using MOPAC [53] (AM1 Hamiltonian with EF minimizer and NOMM correction). Solvation energies, entropy corrections, and ligand reference energies were calculated for all ligands after individual Monte Carlo minimization using specific built-in PrGen modules. Experimental binding affinities were calculated as relative binding affinities using IC_{50} values (RBA = (indirubin IC_{50}/ligand IC_{50}) × 100). It was approximated that $\Delta G \sim -\ln$ RBA. Residues in a range of 12 Å around the ligand were extracted from the receptor PDB file, all water molecules were removed and all hydrogen atoms were added to the receptor.

The 23 minimized ligand molecules comprising the training set were superimposed over the crystallographic position of 6-bromoindirubin 3′-oxime as appears in the pdb file. The ligand equilibration was performed with the following parameters: Tight_coupling = yes/coupling_constant = 1/ corr.coupl.RMS = 0.197/ free_RMS = 0.236. For the Monte Carlo search and minimization during equilibration the parameters were: torsion_window: 15deg/ rotation_w.: 5deg/ transl._w.: 0.5Å/ trials = 15/ conformers = 25/ Minimizer: Powell's_conjugate_gradient_1 /max.cycles = 100 /RMS_of-_forces = 0.1/ energy_change = 10^{-6} /min.step 10^{-6}. To validate the model the 15 molecules of the test set were introduced into the equilibrated receptor that remained fixed during the following process. Ligands were energy-minimized inside the cavity using Monte Carlo search (torsion_window: 90deg./ rotation_w.: 5deg./ transl._w.: 0.5Å/ trials = 15/ conformers = 40). The prediction of their binding affinities was performed by means of the linear regression obtained by the equilibration procedure of the training set:

$$\Delta G_{\text{predicted}} = 0.9608 E_{\text{binding}} + 27.112$$

Calculations were carried out on a Silicon Graphics Indigo R4600 workstation.

Acknowledgment. We are most thankful to Dr. J. Wang for providing the CDK5 and p25 clones and to the fishermen of the "Station Biologique de Roscoff" for collecting the starfish. This research was supported by a grant from the "Association pour la Recherche sur le Cancer" (ARC5732) (L.M.) and a grant from the "Ministère de la Recherche/INSERM/CNRS (Programme Molécules et Cibles Thérapeutiques)" (L.M.). L.M.'s sabbatical leave in Dr. P. Greengard's laboratory was supported by the Rockefeller University and the CNRS.

Appendix

Abbreviations: AD, Alzheimer's disease; AhR, aryl hydrocarbon receptor; BIO, 6-bromoindirubin-3′-oxime; CDK, cyclin-dependent kinase; DTT, dithiothreitol; GSK-3, glycogen synthase kinase-3; IO, indirubin-3′-oxime; I5S, indirubin-5-sulfonate.

References

(1) Cohen, P. The role of protein phosphorylation in human health and disease. *Eur. J. Biochem.* **2001**, *268*, 5001−5010.
(2) Cohen, P. Protein kinases − the major drug target of the twenty-first century? *Nat. Rev. Drug Discovery* **2002**, *1*, 309−315.
(3) Garcia-Echeverria, C.; Traxler, P.; Evans, D. B. ATP site-directed competitive and irreversible inhibitors of protein kinases. *Med. Res. Rev.* **2000**, *20*, 28−57.
(4) Sridhar, R.; Hanson-Painton, O.; Cooper, D. R. Protein kinases as therapeutic targets. *Pharmaceut. Res.* **2000**, *17*, 1345−1353.
(5) Dumas, J. Protein kinase inhibitors: emerging pharmacophores 1997−2000. *Exp. Opin. Ther. Pat.* **2001**, *11*, 405−429.
(6) Manning, G.; Whyte, D. B.; Martinez, R.; Hunter, T.; Sudarsanan, S. The protein kinase complement of the human genome. *Science* **2002**, *298*, 1912−1934.

(7) Malumbres, M.; Ortega, S.; Barbacid, M. Genetic analysis of mammalian cyclin-dependent kinases and their inhibitors. *Biol. Chem.* **2000**, *381*, 827−838.
(8) Malumbres, M.; Barbacid, M. To cycle or not to cycle: a critical decision in cancer. *Nat. Rev. Cancer* **2001**, *1*, 222−231.
(9) Ortega, S.; Malumbres, M.; Barbacid, M. Cyclin D -dependent kinases, INK4 inhibitors and cancer. *Biochim. Biophys. Acta* **2002**, *1602*, 73−87.
(10) Dhavan, R.; Tsai, L.-H. A decade of CDK5. *Nature Rev. Mol. Cell Biol.* **2001**, *2*, 749−759.
(11) Maccioni, R. B.; Otth, C.; Concha, I. I.; Munoz, J. P. The protein kinase Cdk5. Structural aspects, roles in neurogenesis and involvement in Alzheimer's pathology. *Eur. J. Biochem.* **2001**, *268*, 1518−1527.
(12) Smith, D. S.; Tsai, L. H. Cdk5 behind the wheel: a role in trafficking and transport ? *Trends Cell Biol.* **2002**, *12*, 28−36.
(13) Nikoulina, S. E.; Ciaraldi, T. P.; Mudaliar, S.; Carter, L.; Johnson, K.; Henry, R. R. Inhibition of glycogen synthase kinase 3 improves insulin action and glucose metabolism in human skeletal muscle. *Diabetes* **2002**, *51*, 2190−2198.
(14) Eldar-Finkelman, H. Glycogen synthase kinase 3: an emerging therapeutic target. *Trends Mol. Medic.* **2002**, *8*, 126−132.
(15) Kaytor, M. D.; Orr, H. T. The GSK-3β signaling cascade and neurodegenerative disease. *Curr. Opinion Neurobiol.* **2002**, *12*, 275−278.
(16) De Strooper, B.; Woodgett, J. Mental plaque removal. *Nature* **2003**, *423*, 392−393.
(17) Noble, W.; Olm, V.; Takata, K.; Casey, E.; Mary, O.; Meyerson, J.; Gaynor, K.; LaFrancois, J.; Wang, L.; Kondo, T.; Davies, P.; Burns, M.; Veeranna, Nixon, R.; Dickson, D.; Matsuoka, Y.; Ahlijanian, M.; Lau, L. F. and Duff, K. Cdk5 is a key factor in tau aggregation and tangle formation in vivo. *Neuron* **2003**, *38*, 555−565.
(18) Phiel, C. J.; Wilson, C. A.; Lee, V. M.; Klein, P. S. GSK-3alpha regulates production of Alzheimer's disease amyloid-beta peptides. *Nature* **2003**, *423*, 435−439.
(19) Hardcastle, I. R.; Golding, B. T.; Griffin, R. J. Designing inhibitors of cyclin-dependent kinases. *Annu. Rev. Pharmacol. Toxicol.* **2002**, *42*, 325−348.
(20) Knockaert, M.; Greengard, P.; Meijer, L. Pharmacological inhibitors of cyclin-dependent kinases. *Trends Pharmacol. Sci.* **2002**, *23*, 417−425.
(21) Sausville, E. A. Complexities in the development of cyclin-dependent kinase inhibitor drugs. *Trends Mol. Medic.* **2002**, *8*, S32−S37.
(22) Fischer, L.; Endicott, J.; Meijer, L. Cyclin-dependent kinase inhibitors. In *Cell Cycle Regulators as Therapeutic Targets* Meijer, L.; Jézéquel, A.; Roberge, M., Eds., Progress in Cell Cycle Research: Editions "Life in Progress", Station Biologique de Roscoff, 2003; Vol. 5, pp 235−248.
(23) Dorronsoro, I.; Castrob, A.; Martinez, A. Inhibitors of glycogen synthase kinase-3: future therapy for unmet medical needs? *Expert Opin. Ther. Pat.* **2002**, *12*, 1−10.
(24) Martinez, A.; Castro, A.; Dorronsoro, I.; Alonso, M. Glycogen synthase kinase 3 (GSK-3) inhibitors as new promising drugs for diabetes, neurodegeneration, cancer, and inflammation. *Medic. Res. Rev.* **2002**, *22*, 373−384.
(25) Leclerc, S.; Garnier, M.; Hoessel, R.; Marko, D.; Bibb, JA.; Snyder, GL.; Greengard, P.; Biernat, J.; Mandelkow, E,-M.; Eisenbrand, G.; Meijer, L. Indirubins inhibit glycogen synthase kinase − 3β and CDK5/p25, two kinases involved in abnormal tau phosphorylation in Alzheimer's disease − A property common to most CDK inhibitors? *J. Biol. Chem.* **2001**, *276*, 251−260.
(26) Hoessel, R.; Leclerc, S.; Endicott, J.; Noble, M.; Lawrie, A.; Tunnah, P.; Leost, M.; Damiens, E.; Marie, D.; Marko, D.; Niederberger, E.; Tang, W.; Eisenbrand, G.; Meijer, L. Indirubin.; the active constituent of a Chinese antileukaemia medicine.; inhibits cyclin-dependent kinases. *Nat. Cell Biol.* **1999**, *1*, 60−67.
(27) Balfour-Paul, J. *Indigo*; British Museum Press: London, 1998; 1−264.
(28) Cooksey, C. J. Tyrian purple: 6,6′-Dibromoindigo and Related Compounds. *Molecules* **2001**, *6*, 736−769.
(29) Adachi, J.; Mori, Y.; Matsui, S.; Takigami, H.; Fujino, J.; Kitagawa, H.; Miller, C. A. 3rd, Kato, T.; Saeki, K.; Matsuda, T. Indirubin and indigo are potent aryl hydrocarbon receptor ligands present in human urine. *J. Biol. Chem.* **2001**, *276*, 31475−31478.
(30) Gillam, E. M. J.; Notley, L. M.; Cai, H.; DeVoss, J. J.; Guengerich, F. P. Oxidation of indole by cytochrome P450 enzymes. *Biochem.* **2000**, *39*, 13817−13824.
(31) MacNeil, I. A.; Tiong, C. L.; Minor, C.; August, P. R.; Grossman, T. H.; Loiacono, K. A.; Lynch, B. A.; Phillips, T.; Narula, S.; Sundaramoorthi, R.; Tyler, A.; Aldredge, T.; Long, H.; Gilman, M.; Holt, D.; Osburne, M. S. Expression and isolation of antimicrobial small molecules from soil DNA libraries. *J. Mol. Microbiol. Biotechnol.* **2001**, *3*, 301−308.
(32) Tang, W.; Eisenbrand, G. *Chinese drugs of plant origin: chemistry, pharmacology, and use in traditional and modern medicine*; Springer-Verlag: Heidelberg, 1992.
(33) Xiao, Z.; Hao, Y.; Liu, B.; Qian, L. Indirubin and meisoindigo in the treatment of chronic myelogenous leukemia in China. *Leuk. Lymphoma* **2002**, *43*, 1763−1768.
(34) Damiens, E.; Baratte, B.; Marie, D.; Eisenbrand, G.; Meijer, L. Anti-mitotic properties of indirubin-3′-oxime.; a CDK/GSK-3 inhibitor: induction of endoreplication following prophase arrest. *Oncogene* **2001**, *20*, 3786−3797.
(35) Marko, D.; Schätzle, S.; Friedel, A.; Genzlinger, A.; Zankl, H.; Meijer, L.; Eisenbrand, G. Inhibition of cyclin-dependent kinase 1 (CDK1) by indirubin derivatives in human tumor cells. *Br. J. Cancer* **2001**, *84*, 283−289.
(36) Elferink, C. J. Aryl hydrocarbon receptor-mediated cell cycle control. In *Cell Cycle Regulators as Therapeutic Targets*; Meijer, L.; Jezequel, A.; Roberge, M. Eds; Progress in Cell Cycle Research: Editions "Life in Progress", Station Biologique de Roscoff, 2003; Vol. 5, pp 261−267.
(37) Andersson, P.; McGuire, J.; Rubio, C.; Gradin, K.; Whitelaw, ML.; Pettersson, S.; Hanberg, A.; Poellinger, L. A constitutively active dioxin/aryl hydrocarbon receptor induces stomach tumors. *Proc. Natl. Acad. Sci. U.S.A.* **2002**, *99*, 9990−9995.
(38) Bradshaw, T. D.; Trapani, V.; Vasselin, D. A.; Westwell, A. D. The aryl hydrocarbon receptor in anticancer drug discovery: friend or foe? *Curr. Pharmacol. Design* **2002**, *8*, 2475−2490.
(39) Koliopanos, A.; Kleeff, J.; Xiao, Y.; Safe, S.; Zimmermann, A.; Buchler, M. W.; Friess, H. Increased aryl hydrocarbon receptor expression offers a potential therapeutic target for pancreatic cancer. *Oncogene* **2002**, *21*, 6059−6070.
(40) Safe, S.; McDougal, A. Mechanism of action and development of selective aryl hydrocarbon receptor modulators for treatment of hormone-dependent cancers. *Int. J. Oncol.* **2002**, *22*, 1123−1128.
(41) Davies, T. G.; Tunnah, P.; Meijer, L.; Marko, D.; Eisenbrand, G.; Endicott, J. A.; Noble, M. E. M. Inhibitor binding to active and inactive CDK2. The crystal structure of a CDK2-cyclin A/indirubin-5-sulphonate. *Structure* **2001**, *9*, 389−397.
(42) Clark, R. J. H.; Cooksey, C. J. Bromoindirubins: the synthesis and properties of minor components of tyrian purple and the composition of the colorant from *Nucella lapillus*. *J. Soc. Dyers Colour.* **1997**, *113*, 316−321.
(43) Noland, W.; Rieke, R. New synthetic route to 6-nitroisatin via nitration of 3-indolealdehyde. *J. Org. Chem.* **1962**, *27*, 2250−2252.
(44) Vedani, A.; Zbinden, P.; Snyder, J.; Greenidge, P. Pseudoreceptor Modeling: The Construction of Three-Dimensional Receptor Surrogates. *J. Am. Chem. Soc.* **1995**, *117*, 4987−4994.
(45) De Bondt, H. L.; Rosenblatt, J.; Jancaric, J.; Jones, H. D.; Morgan, D. O.; Kim, S. H. Crystal structure of cyclin-dependend kinase 2. *Nature*, **1993**, *363*, 595−602.
(46) Davies, T. G.; Pratt, D. J.; Endicott, J. A.; Johnson, L. N.; Noble, M. E. Structure-based design of cyclin-dependent kinase inhibitors. *Pharmacol. Ther.* **2002**, *93*, 125−133.
(47) Knockaert, M.; Meijer, L. Identifying in vivo targets of cyclin-dependent kinase inhibitors by affinity chromatography. *Biochem. Pharmacol.* **2002**, *64*, 819−825.
(48) Droucheau, E.; Primot, A.; Thomas, V.; Mattei, D.; Knockaert, M.; Richardson, C.; Sallicandro, P.; Alano, P.; Jafarshad, A.; Baratte, B.; Kunick, C.; Parzy, D.; Pearl, L.; Doerig, C.; Meijer, L. *Plasmodium falciparum* glycogen synthase kinase-3, molecular model, expression, intracellular localisation and selective inhibitors. *Biochim. Biophys. Acta* **2003**, in press.
(49) Doerig, C.; Meijer, L.; Mottram, J. C. Protein kinases as drug targets of parasitic protozoa. *Trends Parasitol.* **2002**, *18*, 366−371.
(50) Primot, A.; Baratte, B.; Gompel, M.; Borgne, A.; Liabeuf, S.; Romette, J. L.; Costantini, F.; Meijer, L. Purification of GSK-3 by affinity chromatography on immobilised axin. *Protein Expr. Purif.* **2000**, *20*, 394−404.
(51) Borgne, A.; Meijer, L. Sequential dephosphorylation of p34^{cdc2} on its Thr-14 and Tyr-15 residues at the prophase/metaphase transition. *J. Biol. Chem.* **1996**, *271*, 27847−27854.
(52) Mohamadi, F.; Richards, N. G. J. Guida, W. C.; Liskamp, R.; Lipton, M.; Caufield, C.; Chang, G.; Hendrickson, T.; Still, W. C. MacroModel-An intergrated software system for modeling organic and bioorganic molecules using molecular mechanics. *J. Comput. Chem.* **1990**, *11*, 440−467.
(53) Stewart, J. J. P. MOPAC-a semiempirical molecular orbital program. *J. Comput.-Aided Mol. Des.* **1990**, *4*, 1−105.
(54) Tarricone, C.; Dhavan, R.; Peng, J.; Areces, L. B.; Tsai, L. H.; Musacchio, A. Structure and regulation of the CDK5-p25^{nck5a} complex. *Mol. Cell* **2001**, *8*, 657−669.

JM031016D